The sustainable freight railway: Designing the freight vehicle – track system for higher delivered tonnage with improved availability at reduced cost

SUSTRAIL

Grant Agreement n°: 265740 FP7 - THEME [SST.2010.5.2-2.]
Project Start Date: 2011-06-01
Duration: 48 months

D4.2

SUPPORTIVE BALLAST AND SUBSTRATE

Due date of deliverable: 31/05/2014

Actual submission date: 31/07/2014

Work Package Number:	WP 4
Dissemination Level:	PU
Status:	Final
Leader of this deliverable:	TRAIN
Prepared by:	Donato Zangani, (TRAIN) Clemente Fuggini (TRAIN) Brian Whitney and Kevin Blacktop (NR) Lennart Elfgren, Thomas Blanksvärd, Björn Täljsten, Matti Rantatalo, and Ulla Juntti (LTU) Andrew Arnall, Adam Beagles, and David Fletcher (USFD)
Verified by:	Donato Zangani, (TRAIN)

Dissemination Level	
PU	Public
PP	Restricted to other programme participants (including the Commission Services)
RE	Restricted to a group specified by the consortium (including the Commission Services)
CO	Confidential, only for members of the consortium (including the Commission Services)

Document History			
Version	**Date**	**Author/s**	**Description**
D1	09.06.2014	Donato Zangani et al. from TRAIN	Structure draft and introduction
D2	23.06.2014	Matti Rantatalo et al. from LTU	Contribution to Chapter 6
D3	15.07.2014	Adam Beagle et al. from USFD	Contribution to Chapter 7
D4	22.07.2014	Donato Zangani et al. from TRAIN	Structure update and integration
D5	31.07.2014	Donato Zangani et al. from TRAIN	Verification, editing of the Introduction and conclusions

Disclaimer

The information in this document is provided as is and no guarantee or warranty is given that the information is fit for any particular purpose. The user thereof uses the information at its sole risk and liability.

The document reflects only the author's views and the Community is not liable for any use that may be made of the information contained therein.

EXECUTIVE SUMMARY

For the track itself to maintain its installed geometry for the maximum length of time, it is important that the substrate on which it has been laid is in a homogeneous condition, and remains so as far as is reasonably practicable given other influences such as climatic effects (temperature, groundwater content etc).

Starting from data provided by the Infrastructure Managers involved in the project, deterioration mechanisms of the trackbed were analysed and treatments/recommendations in case of poor stiffness were provided. It is shown as a stiff trackbed results in better track quality with reduced maintenance requirements, resulting in lower whole life cost. Whilst a stiff track bed does result in higher ballast loading, it is clear that this is within acceptable limits and instead other benefits from reduced ballast movement results in less ballast deterioration and therefore increased durability. Very low trackbed stiffness can result in trains approaching the "critical velocity" causing increased ground displacement, unless speed restrictions are introduced this results in rapid deterioration of track geometry.

The effect of trackbed and substructure characterized by variable stiffness was analysed by use of a numerical approach. The attention was given to the role of structures such as bridges and embankments, and track substrate stiffness, in enabling the railway to effectively bear the loads to which it is subjected. A numerical approach was developed for the analysis of the track substructure and the embankment potentially subjected to large deformations and accelerations induced by a running vehicle. Static analyses have shown the effect of soft soil in the embankment structure, which make the embankment more vulnerable to larger deformations concentrated in the subsoil with risk of reduced stability and failure of the shoulder of the embankment. Dynamic analyses have considered the case of a freight vehicle running at different speed and axle load values showing the effect at different depths within the trackbed and in correspondence of transition zones, where the stiffness of the track changes significantly over a short distance. Ground stabilisation and monitoring technologies are introduced based on sensor integrated geogrids which can be embedded into the structure and provide, at the same time, soil stabilisation and structural health assessment functions.

Similarly to what done for trackbed characterized by low stiffness, recommendations on assessment for bridges and their strengthening are given, based on the findings from other European projects. Solutions include the adoption of FRP reinforcement bonded in the intradox of the bridge, showing substantial improvement in terms of the capacity of the structure to sustain the design load, and transition plates, which however did not confirmed the expectations.

Finally, two aspects of track defect damage were considered: the effect of changing support stiffness and the effect of multiple cracks. A Euler–Bernoulli beam model of the rail was used to investigate the effect of varying support stiffness. The model has been used to evaluate the evolution of tensile stress in the rail between vehicles and between wheels on a bogie, and to study how an unsupported sleeper and a transition onto a bridge could affect the bending stresses in rail. The effect of multiple cracks has been studied using a numerical approach based on the Boundary Element Method.

Table of contents

EXECUTIVE SUMMARY **3**

1. INTRODUCTION **7**

2. SITES DATA PROVISION **8**

3. INVESTIGATION ON SITES AND BALLAST DETERIORATION **16**

3.1 TRACK COMPONENTS AND DETERIORATION MECHANISMS 16
3.2 TRACKBED STIFFNESS ASSESSMENT 18
3.2.1 Use of Desk Study Data to Determine whether Formation Stiffness is Adequate *18*
3.2.2 Determination of Dynamic Sleeper Support Stiffness *19*
3.2.3 Treatment of Poor Trackbed Stiffness *20*
3.3 EXAMPLES OF THE RELATIONSHIP BETWEEN STIFFNESS AND TRACK QUALITY 21

4. SUBSTRUCTURE STIFFNESS AND DEFORMATION ANALYSIS **23**

4.1 TRACK AND SUBSTRUCTURE MODELLING 23
4.2 STATIC ANALYSIS OF STRAIGHT RAILWAY TRACK AND SUBSTRUCTURE 24
4.3 DYNAMIC ANALYSES 26
4.4 GROUND STABILIZATION AND MONITORING TECHNOLOGIES 32
4.5 REFERENCES 34

5. UPGRADING SUBSTRUCTURE FOR HEAVIER LOADS **35**

5.1 GENERAL 35
5.2 RECOMMENDATIONS ON ASSESSMENT METHODS FOR BRIDGES 35
5.3 RECOMMENDATIONS ON STRENGTHENING OF BRIDGES 36
5.4 EXPERIENCE OF TRACKS ON BRIDGES AND TRANSITIONS TO BRIDGES 38
5.5 REFERENCES 39

6. TRACK DEFECTS ANALYSIS **42**

6.1 INTRODUCTION 42
6.2 STRESS IN RAILS SUBJECT TO VARYING SUPPORT STIFFNESS 42
6.2.1 Model *42*
6.2.2 Results *43*
6.2.3 Rail Bending Conclusions *47*
6.3 MULTIPLE CRACKS 48
6.3.1 Introduction *48*
6.3.2 Model *48*
6.3.3 Results *50*
6.3.4 Multiple Crack Conclusions *52*
6.4 CONCLUSIONS 52

7. CONCLUSIONS **53**

List of Figures

FIGURE 2.1: MAP OF THE BULGARIAL RAILWAY NETWORK WHERE THE ROUTE SELECTED FOR SUSTRAIL IS HIGHLIGHETD 8
FIGURE 2.2: CROSS-SECTION OF TRACK BETWEEN DIMITROVGRAD-SVILENGRAD KM 249+580 10
FIGURE 2.3: CROSS-SECTION OF TRACK BETWEEN DIMITROVGRAD-SVILENGRAD KM 249+580 (DETAIL) 11
FIGURE 2.4: CROSS-SECTION OF TRACK BETWEEN DIMITROVGRAD-SVILENGRAD KM 253+200 12
FIGURE 2.5: CROSS-SECTION OF TRACK BETWEEN DIMITROVGRAD-SVILENGRAD KM 253+200 (DETAIL) 13
FIGURE 2.6: CROSS-SECTION OF TRACK BETWEEN ELIN PELIN-VAKAREL KM 31+279.95 14
FIGURE 2.7: CROSS-SECTION OF TRACK BETWEEN ELIN PELIN-VAKAREL KM 31+279.95 (DETAIL) 15
FIGURE 3.1: COMPONENTS OF TYPICAL TRACKBED 16
FIGURE 3.2: SUBGRADE EROSION 17
FIGURE 3.3: REQUIRED TOTAL DEPTH OF GRANULAR TRACKBED LAYERS ON COHESIVE SOILS 19
FIGURE 3.4: RELATIONSHIP BETWEEN STIFFNESS AND TRACK QUALITY 21
FIGURE 4.1: SKETCH OF THE TRACK GEOMETRY IN THE TRANSVERSAL SECTION (LEFT); SKETCH OF THE GEOMETRY OF THE FINITE ELEMENT MODELS IN THE TRANSVERSAL SECTION (RIGHT) 24
FIGURE 4.2: SIMPLIFIED MODEL – PURE STATIC ANALYSIS: GEOMETRY AND IMPOSED LOADS 24
FIGURE 4.3: MAGNITUDE OF TOTAL DISPLACEMENTS FOR THE TARE CASE: 1A - SOFT SOIL (LEFT); 1B - STIFF SOIL (RIGHT) 26
FIGURE 4.4: GEOMETRY OF THE CROSS SECTION AT KM 253+200 ALONG THE DIMITROVGRAD-SVILENGRAD RAILWAY LINE IN BULGARIA (LEFT); SECTION ELEMENTS AS MODELLED IN LS-DYNA (RIGHT) 27
FIGURE 4.5: LONGITUDINAL VIEW OF THE CROSS-SECTION: UNMESHED GEOMETRY (LEFT); MESHED MODEL (RIGHT) 28
FIGURE 4.6: DYNAMIC ANALYSIS: CONTOURS OF EFFECTIVE STRESS ALONG TIME (E.G. FOLLOWING THE TRAIN MOVEMENTS) IN THE DIFFERENT LAYERS: SLEEPERS (TOP LEFT); BALLAST (TOP RIGHT); SUB-BALLAST (BOTTOM LEFT) AND SUBSTRATE (BOTTOM RIGHT) 28
FIGURE 4.7: VARIATION OF RESULTANT ACCELERATIONS AT DIFFERENT DEPTHS BELOW THE TRACK (A SUBSOIL, B FORMATION LAYER, C SUB-BALLAST, D BALLAST) AT A CERTAIN LOCATION ALONG THE TRACK INDUCED BY THE TRAIN TRAVELLING AT SPEED V= 70KM/H AND AXLE LOAD =10 T (ABOVE) AND V=140 KM/H AND AXLE LOAD = 22.5 T (BOTTOM) 29
FIGURE 4.8: WHEEL/TRACK CONTACT FORCE ALONG THE TRACK ON LOOSE SAND AS GROUND SOIL FOR DIFFERENT SPEED AND AXLE LOAD, V= 70KM/H AND AXLE LOAD =10 T (ABOVE) AND V=140 KM/H AND AXLE LOAD = 22.5 T (BOTTOM) 30
FIGURE 4.9: ANALYSIS OF BRIDGE-EMBANKMENT SYSTEM 31
FIGURE 4.10: DISTRIBUTION OF EFFECTIVE STRESSES IN THE STRUCTURE: STRESS CONCENTRATIONS ARE LOCALISED IN CORRESPONDENCE OF THE INDIVIDUAL WHEELSET POSITION (ABOVE) AND THREE-DIMENSIONAL COMPLEX STRESS DISTRIBUTION IS OBSERVED IN THE SUBSOIL (BELOW) 31
FIGURE 4.11: WHEEL/TRACK CONTACT FORCE ALONG THE TRACK (ABOVE) AND VARIATION OF RESULTANT ACCELERATIONS AT DIFFERENT DEPTHS BELOW THE TRACK (A SUBSOIL, B FORMATION LAYER, C SUB-BALLAST, D BALLAST) (BELOW) AT A LOCATION CLOSE TO THE TRANSITION ZONE 32
FIGURE 4.12: USE OF GEOTEXTILES FOR SOIL REINFORCEMENT 33
FIGURE 4.13: GEOSYNTHETIC-REINFORCED AND PILE-SUPPORTED EMBANKMENT 33
FIGURE 4.14: MULTIFUNCTIONAL GEOGRID WITH EMBEDDED FIBER OPTICAL DISTRIBUTED SENSOR (AFTER POLYTECT) 34
FIGURE 5.1: THREE PHASES OF ASSESSEMENT OF BRIDGES, SB-LRA, 2007 35
FIGURE 5.2: HIGH LOADS MAY SCRATCH THE BOTTOM OF CONCRETE SLABS AS HERE ON A BRIDGE THAT WAS STRENGTHENED AND TESTED TO FAILURE IN ÖRNSKÖLDSVIK, SWEDEN. PHOTO BY BAM, BERLIN, SUSTAINABLE BRIDGES, 2007; SB7-3, 2008 37
FIGURE 5.3: GROOVES ARE GRINDED IN THE BOTTOM OF A SLAB SO THAT BARS OF CARBON FIBRE REINFORCED POLYMERS (CFRP) CAN BE USED AS NEAR SURFACE MOUNTED REINFORCEMENT (NSMR), SB7-3, 2008. 37
FIGURE 5.4: LOAD-DEFORMATION GRAPHS ACCORDING TO THE TEST AND TO THE FEM MODEL OF THE BRIDGE IN ÖRNSKÖLDSVIK, PUURULA, 2012 38
FIGURE 5.5: TRANSITION SLABS AT SIKÅN BRIDGE, FARA, 2014 38
FIGURE 5.6: INSTALLATION OF TRANSITION SLAB AT SIKÅN BRIDGE, FARA, 2014 39
FIGURE 5.7: MEASUREMENTS BEFORE AND AFTER INSTALLATION OF TRANSITION SLABS AT THE SIKÅN BRIDGE, FARA, 2014 39
FIGURE 6.1: BEAM MODEL OF RAIL 42
FIGURE 6.2: COMPARISON OF SIMPLE AND NON-LINEAR MODELS OF RAIL BENDING 43
FIGURE 6.3: RAIL BENDING WHEN ONE SLEEPER IS UNSUPPORTED 44

FIGURE 6.4: RAIL BENDING WHEN TWO SLEEPERS ARE UNSUPPORTED 45
FIGURE 6.5: VEHICLE PASSING OVER TRANSITION TO STIFF SUPPORT 46
FIGURE 6.6: VEHICLE PASSING OVER RAMPED TRANSITION TO STIFF SUPPORT 47
FIGURE 6.7: EXAMPLES OF RCF DAMAGE FROM RAILTRACK'S "RAIL FAILURE HANDBOOK" RT/CE/S/057, 2001 48
FIGURE 6.8: CRACK MODELS 49
FIGURE 6.9: STRESS INTENSITY FACTORS FOR SINGLE CRACKS AT DIFFERENT ANGLES 50
FIGURE 6.10: STRESS INTENSITY FACTORS FOR CRACKS AT LEFT-HAND END OF GROUP 50
FIGURE 6.11: STRESS INTENSITY FACTORS FOR CRACKS IN MIDDLE OF GROUP 51
FIGURE 6.12: STRESS INTENSITY FACTORS FOR CRACKS AT RIGHT-HAND END OF GROUP 51
FIGURE 6.13: STRESS INTENSITY FACTORS FOR CRACKS IN GROUP OF ELEVEN 52

List of Tables

TABLE 3.1: REQUIRED DYNAMIC SLEEPER SUPPORT STIFFNESS 18
TABLE 4.1: TRAIN, SUPERSTRUCTURE AND SUBSTRUCTURE COMPONENTS 25
TABLE 4.2: SCENARIOS IMPLEMENTED IN THE PURE STATIC ANALYSIS 25
TABLE 4.3: SELECTED SOIL MATERIALS USED IN THE SIMULATIONS AND ELASTIC CONSTANTS 29

1. INTRODUCTION

The current deliverable has been produced as results of the activities carried out within Task 4.2 "Supportive ballast and substrate" of the Sustrail project, leaded by TRAIN. The objective of the task is to identify the impacts of substrate stiffness variation on track geometry deterioration and other track defects such as the effect of vertical plane long wavelength rail bending on rolling contact fatigue crack growth. The activities have focused on the role of structures such as bridges and embankments, and track substrate stiffness, in enabling the railway to effectively bear the loads to which it is subjected.

The work has been split into 6 subtasks. Subtask 4.2.1 "Sites data provision" leaded by the infrastructure managers, focused on data collection on track and ballast stiffness at various relevant sites on railways used for freight including data on high speed lines. Some details of this work are reported in Chapter 2.

Subtask 4.2.2 "Investigation on sites and ballast deterioration" leaded by Network Rail, aimed at gathering data on deterioration of track geometry and ballast stiffness comparing different routes and analysing sharp changes in deterioration along a route section. Recommendations from this subtask are presented in Chapter 3 of this report.

Subtask 4.2.3 "Substructure stiffness and deformation analysis" leaded by TRAIN, aimed at developing a numerical approach for the analysis of the status of the track substructure subjected to different loading conditions (e.g. corresponding to different axle loads and speed of the freight vehicle) and characterised by different soil components. The results of this work is summarised in Chapter 4.

Subtask 4.2.4 "Sensing methods for loading effects" leaded by University of Newcastle, with the objective to create a low-cost, portable system that can be used for monitoring train-track interaction, and that can be implemented on the track without the need close the line.

Subtask 4.2.5 "Upgrading substructure for heavier loads" leaded by Lulea University, focused on advanced assessment and strengthening methods for bridges and transitions zones to bridges. Some findings and references from other research projects focused on such aspects are reported in Chapter 5.

Finally Subtask 4.2.6 "Track defects analysis" leaded by University of Sheffield aimed at assessing the effect on rolling contact fatigue crack growth of vertical plane long wavelength rail bending using a numerical approach. The results of this work are presented in Chapter 6.

Brief conclusions are reported at the end of the report.

2. SITES DATA PROVISION

Subtask 4.2.1 "Sites data provision" leaded by the infrastructure managers, focused on data collection on track and ballast stiffness at various relevant sites on railways used for freight including data on high speed lines.

Among the data provided we report hereafter the details from the Bulgarian route since it was selected to be considered for the numerical simulations carried out in Subtask 4.2.3 and hereby described in Chapter 4.

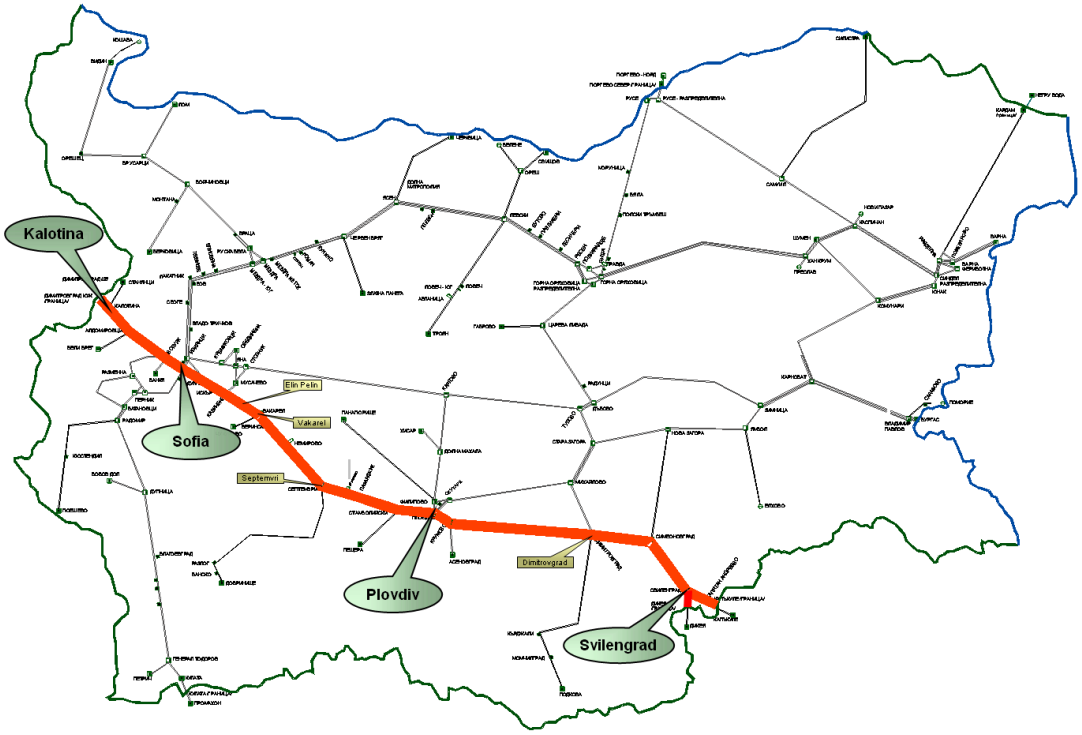


Figure 2.1: Map of the Bulgarial railway network where the route selected for SUSTRAIL is highlighetd

Figure 2.1 above shows the map of the railway network of Bulgaria. Highlighted in red is the route selected for SUSTRAIL which runs between the Serbian border (Kalotina in Bulgaria, by Dimitrovgrad in Serbia) and the Turkish border (Svilengrad in Bulgaria, by Kapikule in Turkey). Further details on this route are provided in deliverable D1.2 "Overview of route and track parameters". This route is interesting for the project not only because is a mixed route for freight and passenger transportation and because of the strategic position for the transportation of goods across Bulgaria, but also because of issues which characterise this route which could potentially found solutions from the SUSTRAIL innovations.

Figure 2.2 shows the cross section of the route between Dimitrovgrad and Svilengrad. Figure 2.3 shown a detail of the sction. The site is located along the railway line /Sofia – Septemvri – Plovdiv/ in Elin Pelin – Vakarel open line and represents a drainage of the doubled railway line in the section from km 31+207 to km 31+575 with length of 368 m. Track №2 was built later than track №1 during doubling of the line.

The situation of the line in this section is in a north curve (having in mind increasing distance in kilometers) and Track №1 is with a radius of 300 m and Track №2 is with radius of 300 m.

The longitudinal inclination is 23,80‰ from km 31+050 to km 31+350, and from km 31+350 to km 31+850 it is 22,12‰.

The superstructure is supported jointed track type with rails 49 kg/m and sleepers CT-6 of elastic fastening SKL14.

In consequence of snow melting and of heavy rains in the last years, more often in spring, presence of water and tempering of the ballast prism between both tracks and especially around the internal rail of Track № 2 have been observed. This provokes unsteady subsiding and falling down of Track №2 from km 31+207 to km 31+575. It causes disturbance of vehicle traffic safety in this section and determines decrease of their speed to 40 km/h.

To solve this problem, construction of a drainage between both tracks is envisaged (perforated PVC tube Ø110 mm, laid down on padded concrete, filled up with river washed gravel) in compliance with the attached characteristically cross profile.

Figure 2.4 shows the cross section of the route between Dimitrovgrad and Svilengrad at km 253+200; Figure 2.5 shows a detailed view of the section. Figure 2.6 shows the cross section of the route between Elin Pelin and Vakarel at km 31+279.95 and Figure 2.7 shows a detailed view of the section. These sections are representative of locations where the construction of a water impermeable layer is being considered.

Protective water impermeable layer is applied only as an exception in the following cases:

- in case of a requirement for higher level of the drainage facilities;
- in case of needed protection of the existing ditches' angle of repose;
- with the purpose of excavation works limitation in case of new construction.

It should be constructed from uncombined materials (crushed stones, ballast, secondary stone material and etc.) with granulometric composition 0-16 mm. Water permeability factor should be less than 0,005 m/24 hours. Water impermeability is ensured through addition of materials with size of fractions less than 0,02 mm (stone flour, cement and etc.) in quantities over 3% or polymer fillers.

The protective layer may be constructed from some constructive layers, as the upper one is 10-15 cm in depth in order to be water impermeable.

The protective layer covers the overall width of the base ground bed in an excavation, as the level of the upper surface should not be lower than the upper edge of the drainage facilities (ditches and trenches).

The base ground bed, on which the protective layer is laid down, is shaped with cross declination of 5%.

The structure, type of used materials and technology of performance are determined in an individual design and the particular solutions are verified in experimental sections.

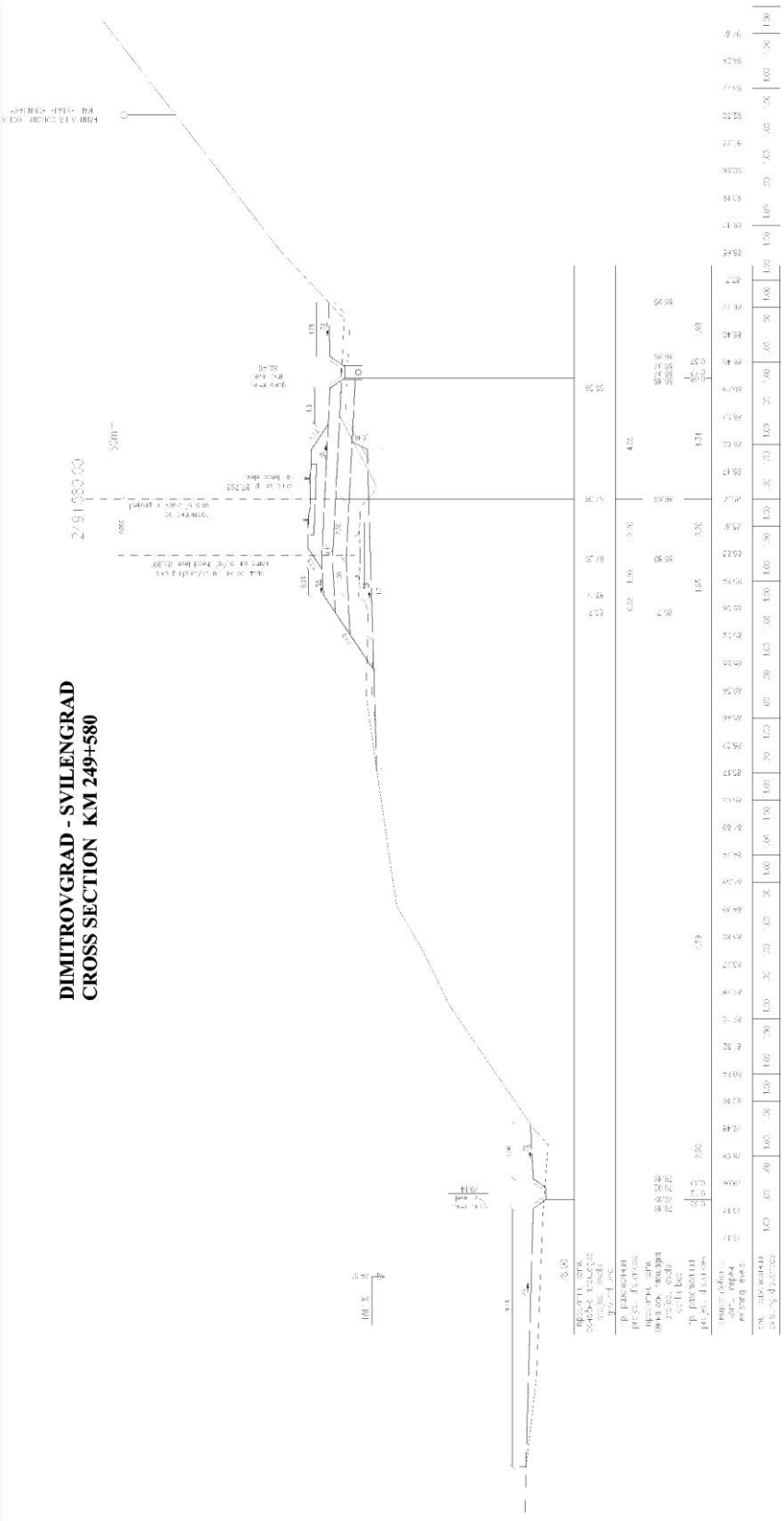


Figure 2.2: Cross-section of track between Dimitrovgrad-Svilengrad km 249+580

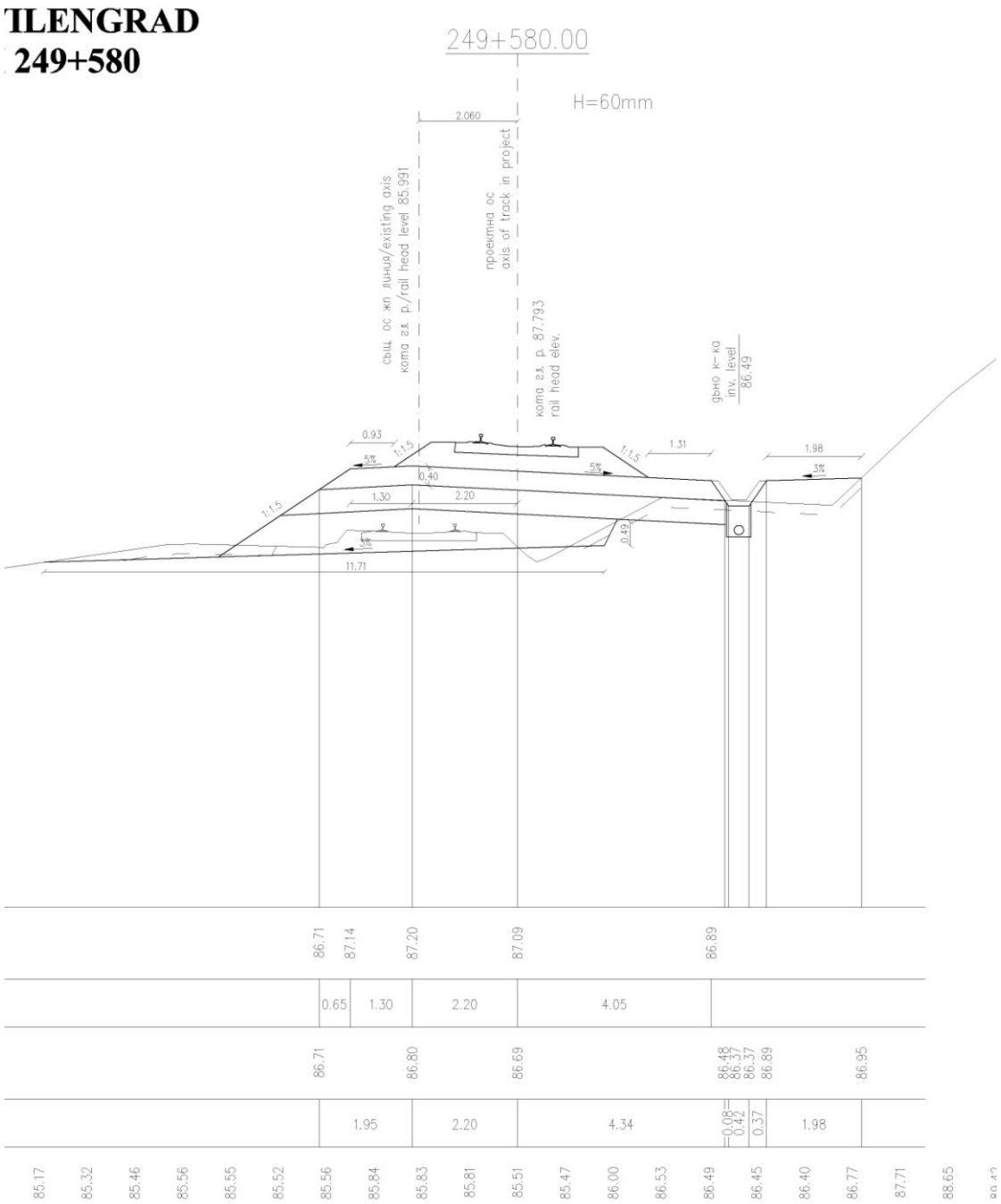


Figure 2.3: Cross-section of track between Dimitrovgrad-Svilengrad km 249+580 (detail)

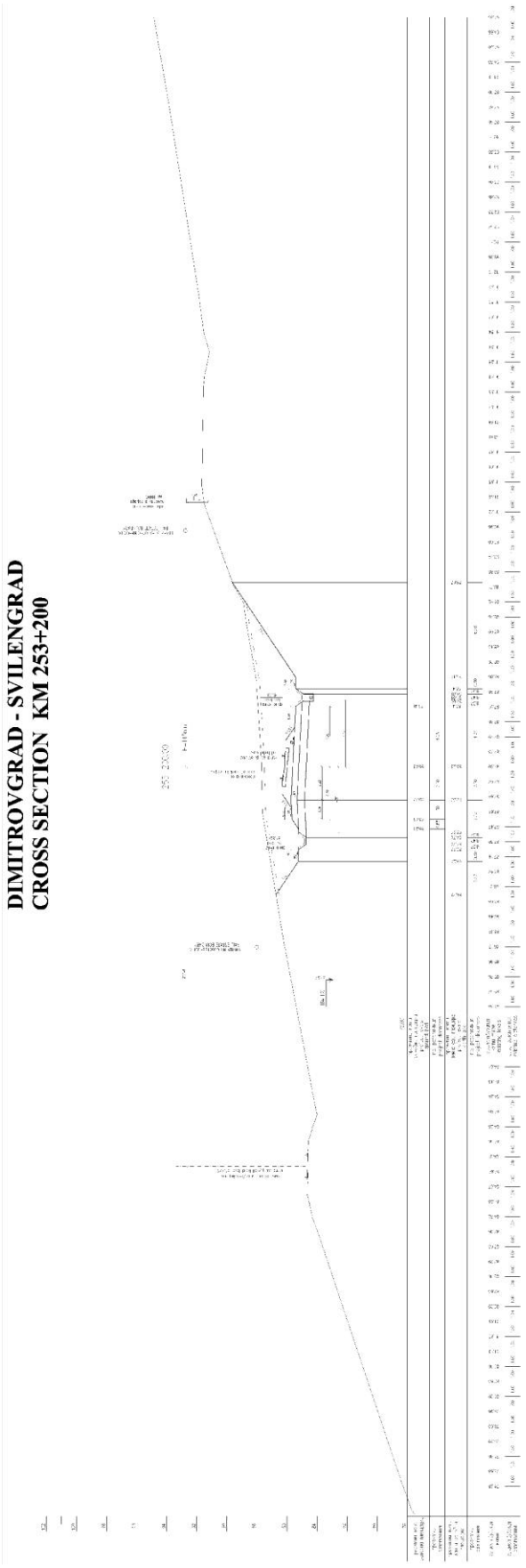


Figure 2.4: Cross-section of track between Dimitrovgrad-Svilengrad km 253+200

DIMITROVGRAD - SVILENGRAD
CROSS SECTION KM 253+200

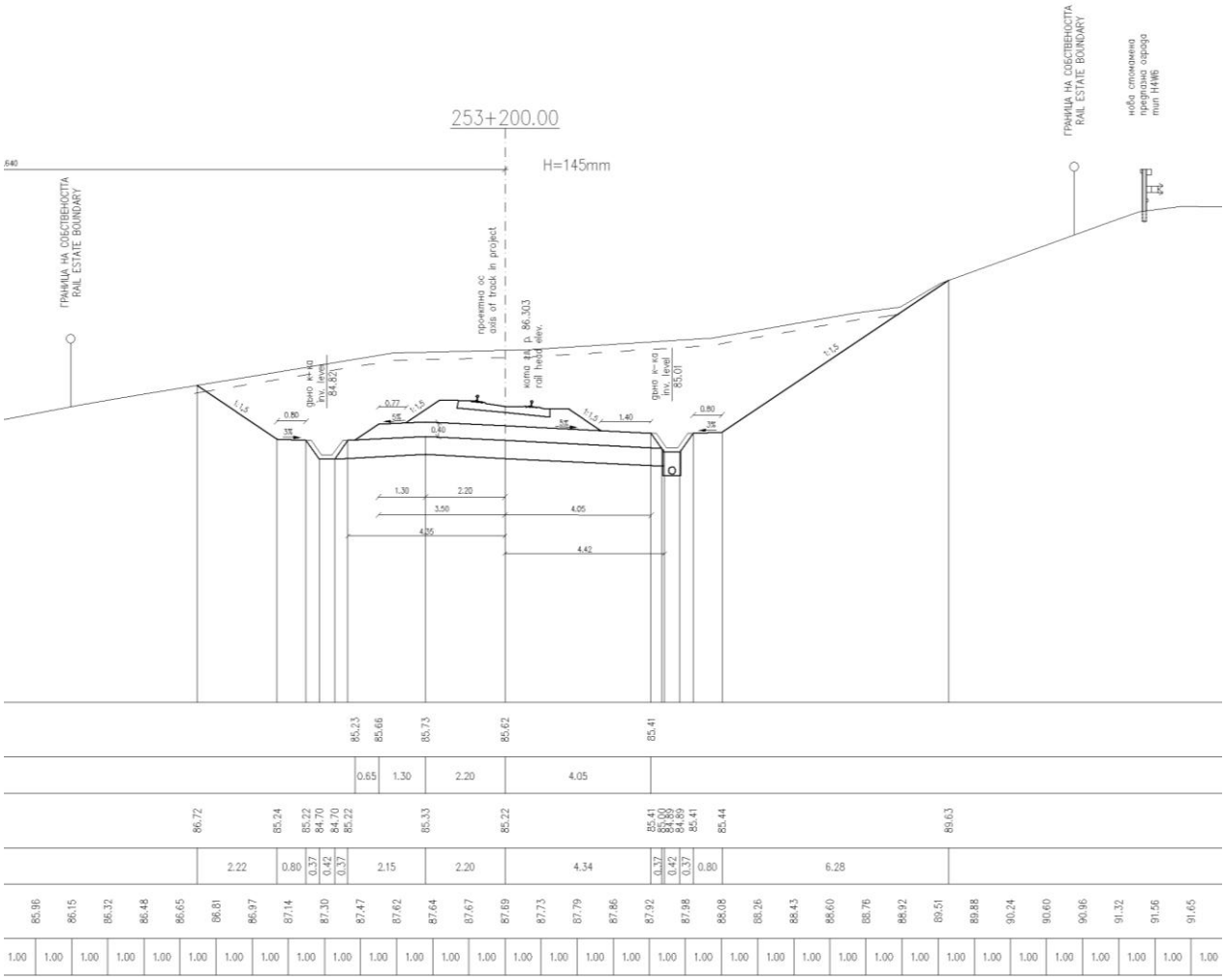


Figure 2.5: Cross-section of track between Dimitrovgrad-Svilengrad km 253+200 (detail)

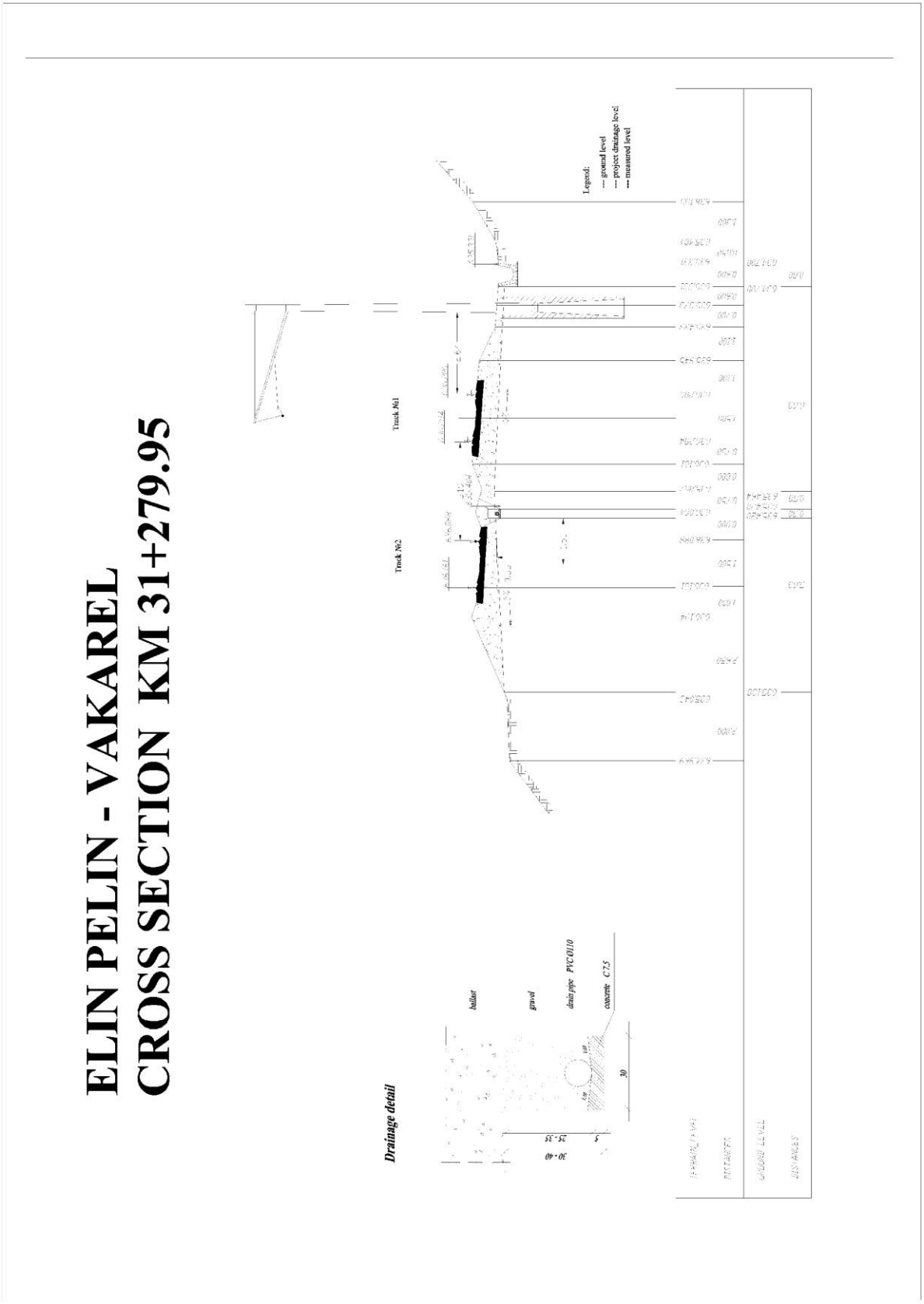


Figure 2.6: Cross-section of track between Elin Pelin-Vakarel km 31+279.95

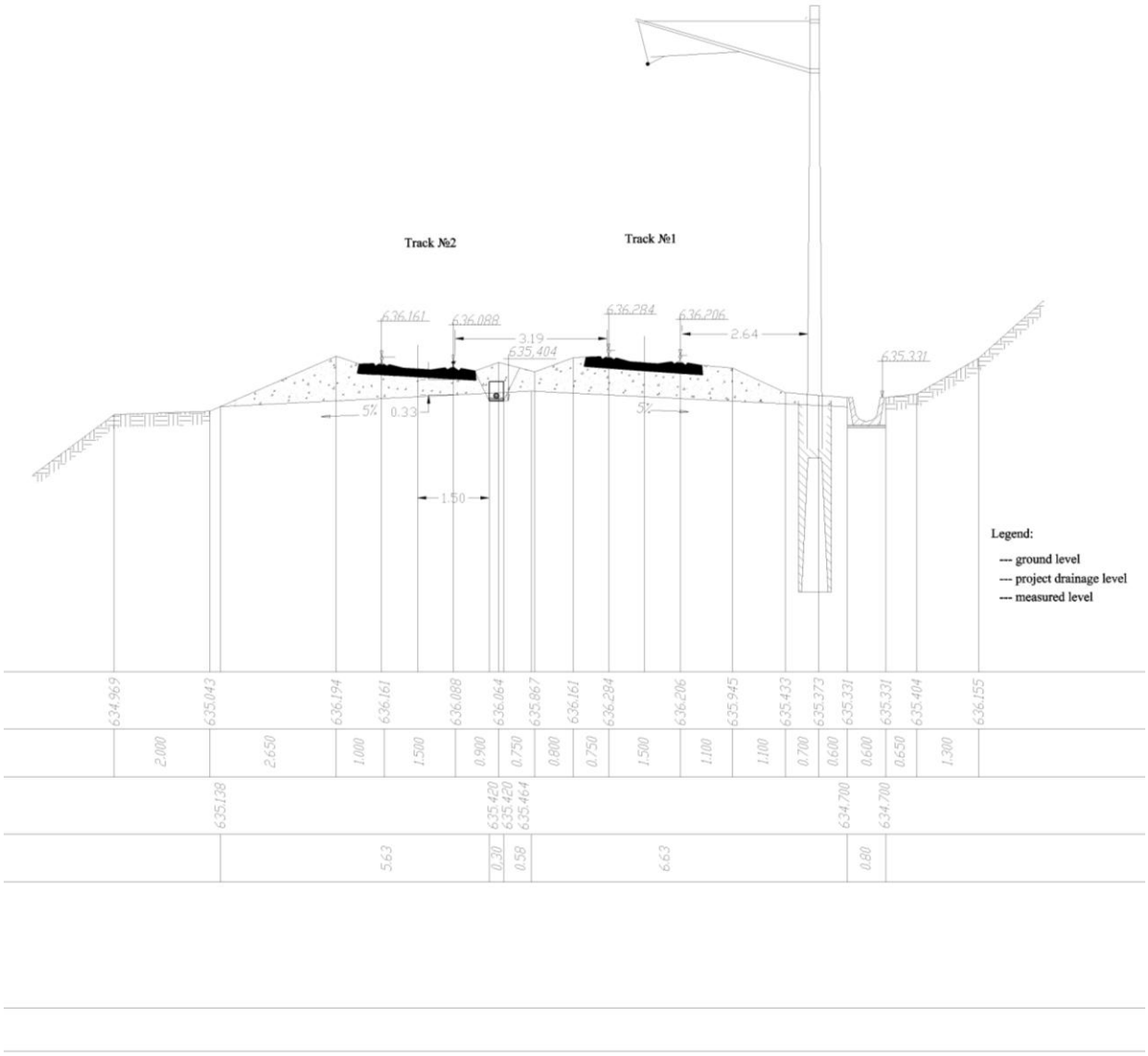


Figure 2.7: Cross-section of track between Elin Pelin-Vakarel km 31+279.95 (detail)

3. INVESTIGATION ON SITES AND BALLAST DETERIORATION

3.1 Track components and deterioration mechanisms

The quality of a track, i.e. its ability to retain good geometry and its response to mechanical maintenance (tamping, stone blowing) is directly related to the design and condition of the trackbed and earthworks.

The trackbed is normally considered to consist of two elements:

- The ballast, which allows for adjustment of the line and level of the track. Ballast deteriorates with traffic passing and with track maintenance activities and therefore requires occasional replacement.
- The formation, consisting of blanket (if present) and subgrade, upon which the required depth of ballast is placed. Ideally this should be permanent, and not require replacement or maintenance.

On a well built formation the only trackbed treatment required should be ballast replacement. However, there are many formations which do not provide the ideal support conditions, and can therefore lead to a considerable reduction in the useful life of the trackbed and high maintenance requirements.

Figure 3.1 illustrates the terminology used to describe the components of a typical trackbed.

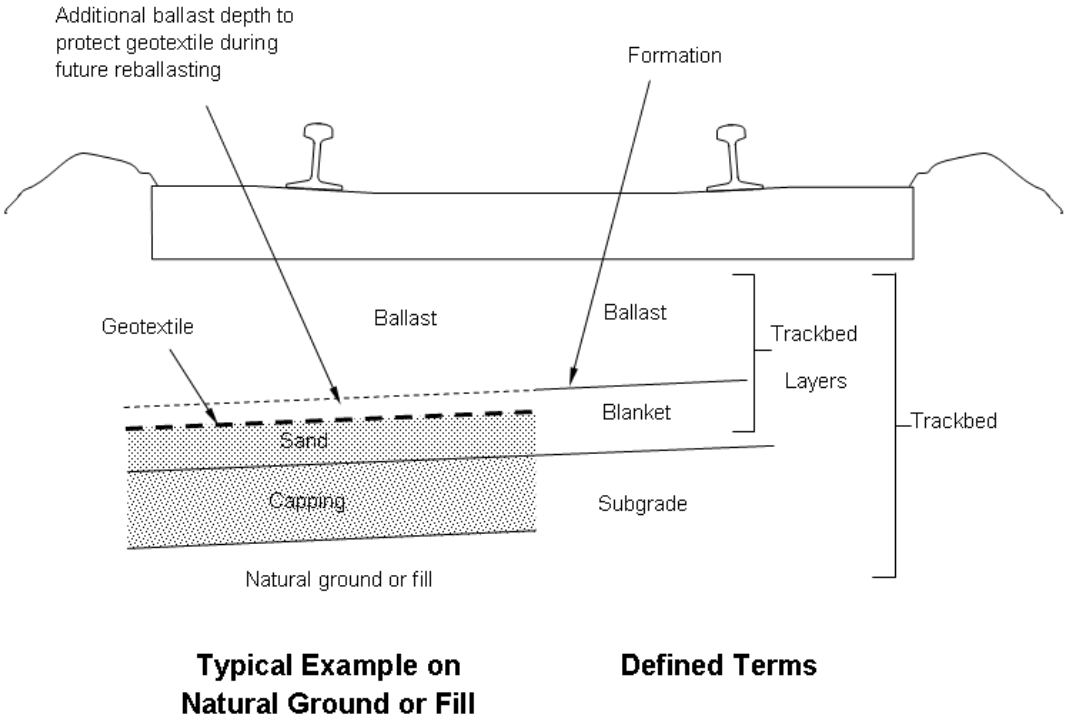


Figure 3.1: Components of typical trackbed

Various mechanisms can result in poor track geometry. These can be divided into five main categories:-

- Ballast deterioration - Ballast should be clean, free draining, resistant to settlement and respond well to maintenance. In-service ballast breaks down gradually under the action of traffic and mechanical maintenance until the voids eventually become filled with fines.
- Subgrade Erosion (pumping) – This occurs when water rises into the ballast layer under the action of train loading and is often highlighted by the appearance of wet beds or spots.
- Subgrade Strength Failure (cess heave) - This is characterised by the development of a continuous failure surface between the base of the trackbed layers and the ground surface. Heaving of the ground surface can occur on both sides of the track foundation although the final movement occurs only on one side (normally the cess, because it is lower than the six-foot), accompanied by loss of level of one rail.
- Poor Stiffness Characteristics - Ballast stability requires a stiff trackbed. Research shows that soft support will result in large ballast settlements. Trackbed stiffness is an important factor from the point of view of track quality. Where there are chronic problems in track geometry it is important to establish whether poor stiffness characteristics may be a contributory cause, particularly in the case of transitions.
- Critical velocity - On very soft ground the stiffness of the trackbed varies with train speed and may reduce considerably at high speeds. This phenomenon is associated with a low velocity of surface wave propagation. As the trains approach the "critical velocity" the ground displacement increases. In extreme cases it may not be possible to run the trains at line speed without causing rapid deterioration of track geometry.



Figure 3.2: Subgrade Erosion

Table 3.1 gives the required dynamic sleeper support stiffness for different lines. These are the minimum values that need to be provided to guarantee that the track quality can be maintained to an adequate standard.

Table 3.1: Required Dynamic Sleeper Support Stiffness

		Minimum Dynamic Sleeper Support Stiffness (K) - kN/mm/sleeper end (Figures in brackets show Failing Weight Deflectometer sleeper deflection in mm – 12 tonne peak load)
Absolute Value		30 (2.0)
Existing Main Lines	With Geogrid Reinforcement	30 (2.0)
	Without Reinforcement	60 (1.0)
Greenfield Sites	Up to 100mph	60 (1.0)
	Above 100mph	100 (0.6)

Where poor stiffness is identified in a site investigation, a low cost compromise solution is to install a geogrid, which will compensate for poor formation stiffness, i.e. it will reduce ballast settlement and hence reduce the rate of deterioration of track quality.

Under certain circumstances it will be necessary to increase total thickness of trackbed layers (ballast plus blanket), particularly at a transition. Note - the total thickness of trackbed layers that is required to distribute the load over the subgrade should not be confused with the required depth of ballast, which determines trackbed life.

3.2 Trackbed Stiffness Assessment

This section describes the procedure for checking whether trackbed stiffness is adequate for the line category, and what options there are available for either improving or compensating for poor stiffness.

The first stage in the process is to examine the historical track quality and maintenance data for the site. Where there has been difficulty in achieving the required track geometry in the past the stiffness characteristics of the trackbed and subgrade should be assessed, either by deep investigation or by shallow investigation plus direct in situ measurement of formation stiffness.

3.2.1 Use of Desk Study Data to Determine whether Formation Stiffness is Adequate

Where track geometry has consistently been good without excessive maintenance requirements, it is reasonable to assume that the stiffness characteristics (and hence the required depth of trackbed layers) are acceptable, provided that the following conditions apply:

- there are no underlying reasons to suspect that the subgrade stiffness has been affected, for example by earthwork failures;

- no significant track lowering (no more than 50mm) is planned as part of the track scheme;
- the blanket or pitching (where present) is in good condition and will not be disturbed by any proposed treatment.

3.2.2 Determination of Dynamic Sleeper Support Stiffness

If the desk study cannot confirm that the stiffness of the trackbed is adequate, it shall be determined by investigation. It shall be noted that rail mounted systems that measure track stiffness are acceptable as a broad brush technique for identifying areas with track stiffness problems, they do not necessarily provide information on trackbed stiffness. Track stiffness is is a function not only of trackbed condition, but also of sleepers, railpads and any voiding that may have developed. The stiffness of the trackbed shall either be assessed by an intrusive investigation of the trackbed layers and subgrade or by direct measurement using the Falling Weight Deflectometer (FWD).

Intrusive Trackbed Investigation

Where it is necessary to check that the Formation Stiffness is adequate this shall normally be addressed in the trackbed investigation. Sufficient deep investigation shall be undertaken, targeted at areas of poor top and or high maintenance requirements, to establish the nature of the subgrade, its strength (if clay or silt) and the degree and depth of weathering.

On cohesive soils an approximation of the sleeper support stiffness can be derived from Figure 3.3 using a description of the consistency of the soil (ideally supplemented by values of undrained shear strength,C_u) and the total depth of granular material below the sleeper.

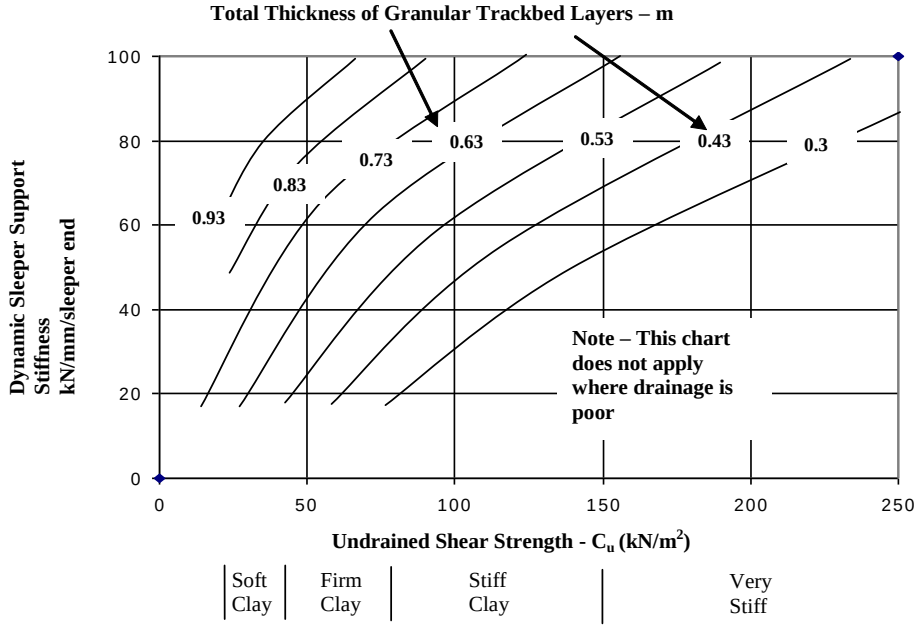


Figure 3.3: Required total depth of granular trackbed layers on cohesive soils

Use of Light Weight Deflectometer (LWD) to Measure Formation Stiffness
It is possible to measure formation stiffness in a trial pit using directly using the LWD. For design purposes it is important that the stiffness values shall be measured at a level of 300mm below proposed base of sleeper. Note, Formation stiffness values quoted as 15, 30 and 45MN/m^2 correspond to K values of 30, 60 and 100 kN/mm/sleeper end respectively.

Assumptions where Drainage is Poor
Figure 3.3 refers only to trackbeds having either good or satisfactory drainage. It does not apply to trackbeds with poor drainage because saturated granular layers may give a low formation stiffness under dynamic loading. If it is impracticable to install a drainage system with an invert either 50mm below the base of the granular layers or 0.5m below base of sleeper, the value of K given in Figure 3.3 should be divided by two for design purposes.

Falling Weight Deflectometer
In critical areas, where it is deemed necessary to make direct measurements and understand the extent of soft formation the Falling Weight Deflectometer shall be used. Areas deemed to require FWD surveys shall include:-

- Sections of track where investigation has indicated frequent values of K which are significantly below 30kN/mm/sleeper end;
- Transition zones where it is necessary to identify the cause of poor track quality;
- Areas where Critical Velocity is thought to be an issue, or is likely to become a problem after route upgrading.

3.2.3 Treatment of Poor Trackbed Stiffness

The following solutions apply only to sites where critical velocity is not an issue.

Geogrid Reinforcement
Geogrids are most effective where the formation is soft, but have a decreasing effect on stiff formation.
Where the absolute minimum value of K can be sensibly achieved throughout a site on an existing line where the "Existing Main Line" value is required, a geogrid shall be used to compensate for low stiffness, placed directly below the ballast, i.e on top of the formation or any geotextile.

Proof Rolling of Existing Formation
Where the formation consists of a well drained granular blanket at least 200mm thick the site shall be proof rolled to maximise trackbed stiffness.

Increase in Construction Depth
Where the absolute minimum value of K (or the equivalent formation stiffness as determined with the LWD) cannot be achieved, the depth of construction shall be increased. Various options are available for stiffening a formation, many of which include non-granular materials.
The simplest option, i.e. placing new well compacted granular layer(s) can be designed using Figure 3.3 If the required depth of granular material below the ballast is less than 200mm, blanketing sand shall be installed. Where greater depths are required, a trackbed specialist shall be consulted.

If the subgrade is non cohesive or no direct measurements of undrained shear strength are possible, an equivalent value can be obtained from with Dynamic Cone Penetrometer(DCP) tests or Standard Penetration Tests (SPT), where available, using the recognised conversion factors.

3.3 Examples of the relationship between Stiffness and Track Quality

An investigation was carried out on serious critical velocity problem on a UK route that resulted in a significant speed restriction. A trackbed investigation had shown that the there was a hard spot at due to a shallow culvert, but that most of the site consisted of soft clay. The rate of deterioration of track quality in the area had been very high. At this stage the problem was thought to be due largely to the transition between the hard culvert and the soft formation, yet it was soon observed that the speed reduction led to a significant reduction in the rate of deterioration of track quality. The problem was related to a low critical velocity, which was confirmed by the FWD testing. Ground wave velocity through the trackbed in this area was about 50m/s compared to about 100m/s elsewhere. Sleeper deflections were also greater in this area, with over 2mm being recorded, compared to less than 1mm on other parts of the route.

Following an extensive rebuild the trackbed stiffness and critical velocity was raised allowing full line speed to be reinstated and with reduced on-going maintenance. This resulted in an approximate 35% improvement in trackbed efficiency, from the point of view of minimising ballast displacement at high speed.

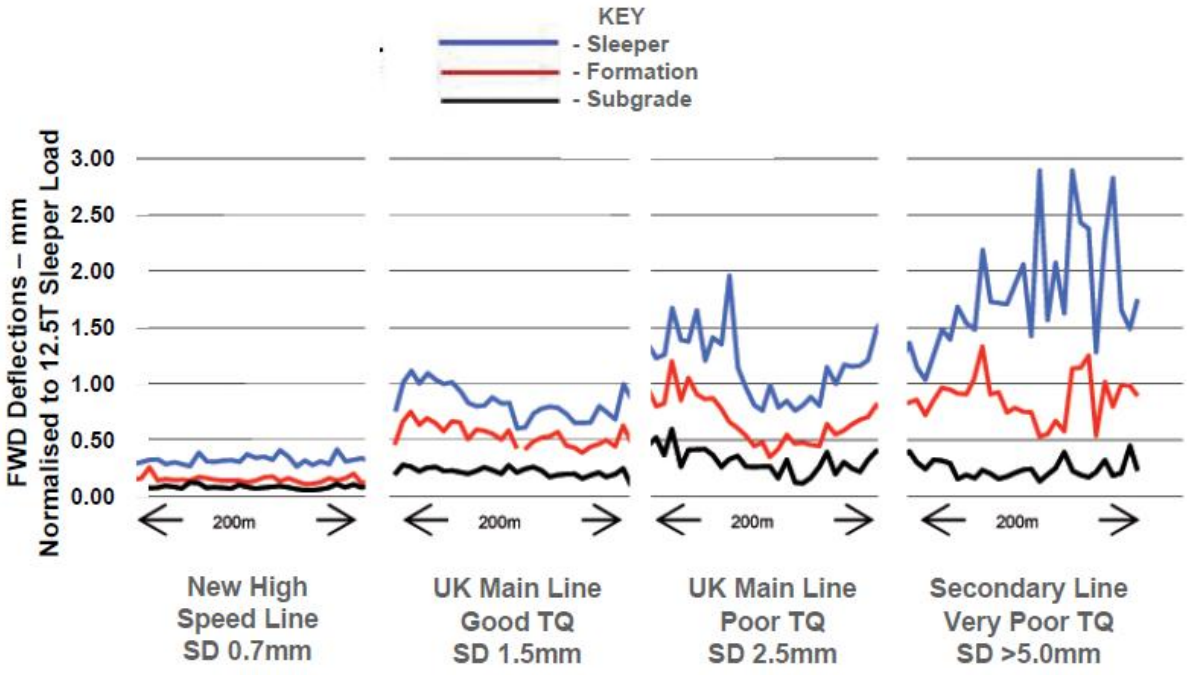


Figure 3.4: Relationship between Stiffness and Track Quality

3.4 Conclusions

A stiff trackbed results in better track quality with reduced maintenance requirement, resulting in lower whole life cost. Whilst a stiff track bed does result in higher ballast loading as

demonstrated in SUSTRAIL 4.1, it is clear that this is within acceptable limits and instead other benefits from reduced ballast movement results in less ballast deterioration and therefore increased durability.

Very low trackbed stiffness can result in trains approaching the “critical velocity” causing increased ground displacement, unless speed restrictions are introduced this results in rapid deterioration of track geometry

4. SUBSTRUCTURE STIFFNESS AND DEFORMATION ANALYSIS

4.1 Track and substructure modelling

The aim here was to develop a numerical approach for the analysis of the track substructure and the embankment potentially subjected to large deformations and accelerations induced by a running vehicle. We were also interested for a numerical codes that allows implementing a variety of material models and constitutive laws.

A static analysis was first carried out to study the global response of the railway track to the imposed loads from a freight vehicle. This allows setting up a baseline for more complex (e.g. dynamic) analyses, since in principle the static model provides as output the field of deformations in the substructure for different freight vehicles (i.e. different loads and speeds) and different soil characteristics. The commercial software ANSYS was selected for the static analysis and pure static as well pseudo-static (transient) analysis were carried out, whose results are briefly reported hereafter.

Dynamic analyses were then carried out to understand the interaction among the load imposed from a vehicle running at different speeds and with variable axle load and the substructure response at different critical locations. Different soil parameters for the substructure were considered as well. The commercial software LS-Dyna was used for this purpose, which allows for explicit time integration.

The static analysis (both pure static and pseudo-static) have been carried out with a simplified model of the railway infrastructure, whilst the dynamic analysis has been carried out considering more complex geometry and has been also extended to study the effects of a large variation of the substructure stiffness, like in presence of a bridge-embankment transition zone.

The finite element models prepared for the static and dynamic analyses have the following characteristics:

- the superstructure is composed of rails and sleepers;
- the substructure is composed of the ballast, the sub-ballast and the subgrade;
- a 3D spatial model is conceived: the model represents a segment of a straight railway track section;
- the track is embedded in a layered substructure;
- linear material models are initially considered;
- all structural elements (rail, sleepers, ballast, subgrade) are discretized using solid (brick) elements;
- contact areas are modelled as homogeneous and contact properties do not change in time;
- different vehicle speeds are considered: 70 kph, 120 kph and 140 kph;
- two loading configurations for the vehicle are considered: tare (5t) and laden (21t);
- different soil conditions are considered: soft and stiff clay and loose and dense uniform sand.

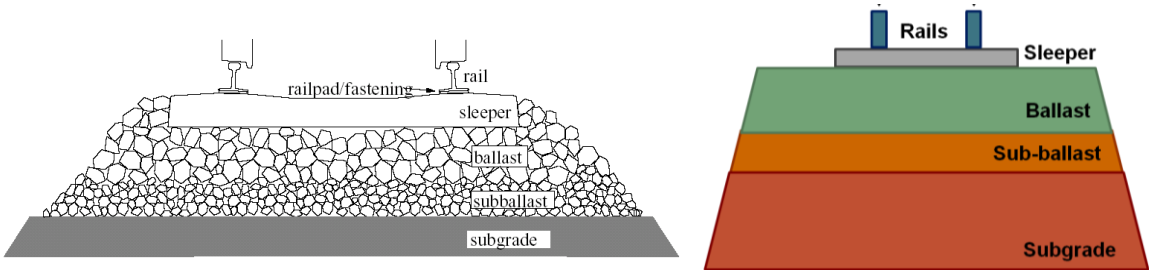


Figure 4.1: Sketch of the track geometry in the transversal section (left); Sketch of the geometry of the Finite Element Models in the transversal section (right)

4.2 Static analysis of straight railway track and substructure

The finite element model prepared for the static analyses is representative of a section of railway track of 36.2 metres length; half of the track is modelled explicitly for the symmetry conditions. The train is loading the track with a vertical static force, calculated from the axle load (5t in the tare case and 21t in the laden case). In the pseudo-static analysis, the wheel of the train (steel made) has been explicitly modelled as a rigid body moving at a certain speed.

The superstructure is made of rails and sleepers. Rails (UIC 60) are modeled with an isotropic elastic material and have a rectangular cross section being equivalent to the I shape section. Sleepers are modelled as rigid elements made of concrete with rectangular cross section. Half a sleeper is modelled having a mass of 125kg. The model is constrained such as displacements are restrained orthogonal to the lateral boundaries of the model; the bottom part of the subgrade is constrained in all degrees of freedom (no vertical and horizontal movements).

The geometry of the model is shown in the next picture where the effect of the train (two wagons, four bogies) is represented as concentrate vertical loads (vertical forces) at given locations.

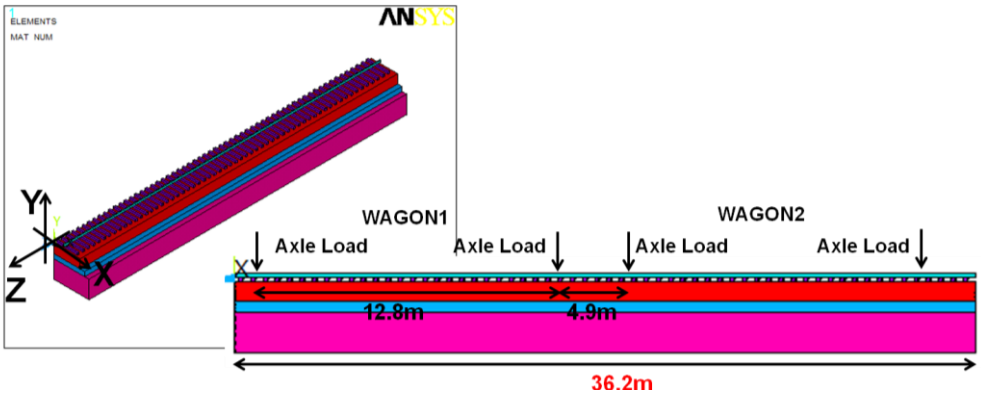


Fig. 4

Figure 4.2: Simplified model – Pure Static Analysis: geometry and imposed loads

The substructure is made of 3 layers corresponding to (from top to bottom): the ballast, the sub-ballast and the subgrade as depicted in the above picture. Each layer is modelled with an isotropic elastic material. The main material properties are reported in the table below.

Table 4.1: Train, Superstructure and Substructure components

Component	Parameter	Value
Wheel	Mass	750 Kg
	Density	7850 Kg/m^3
	Young Modulus	210000 MPa
Track	Total Length	36.2 m
Rail	Dimensions (H*W)	200*50 mm
	Density	7850 Kg/m^3
	Young Modulus	210000 MPa
Concrete Sleeper	Spacing	0.6 m
	Dimensions (L*H*W)	2.5*0.2*0.2 m
Ballast	Dimensions (H*W)	1*3 m
	Density	1600 kg/m3
	Elastic Modulus	350 MPa
Sub-ballast	Dimensions (H*W)	0.5*3.5 m
	Density	1900 kg/m3
	Elastic Modulus	100 MPa
Subgrade	Dimensions (H*W)	2*4 m
	Density	2000 kg/m3
	Elastic Modulus	10 – 80 MPa

The main objective here is to study the effects of the train load on the railway infrastructure for different loading conditions (tare and laden) and different soil (e.g. subgrade) characteristics (soft and stiff). To this aim, the following scenarios have been implemented.

Table 4.2: Scenarios implemented in the pure static analysis

Subgrade Characteristics Train Configuration	Soft Soil	Stiff Soil
Tare (5t)	1a	1b
Laden (21t)	2a	2b

Next picture shows the results of the simulations for the tare case scenario in terms of magnitude of total displacements.

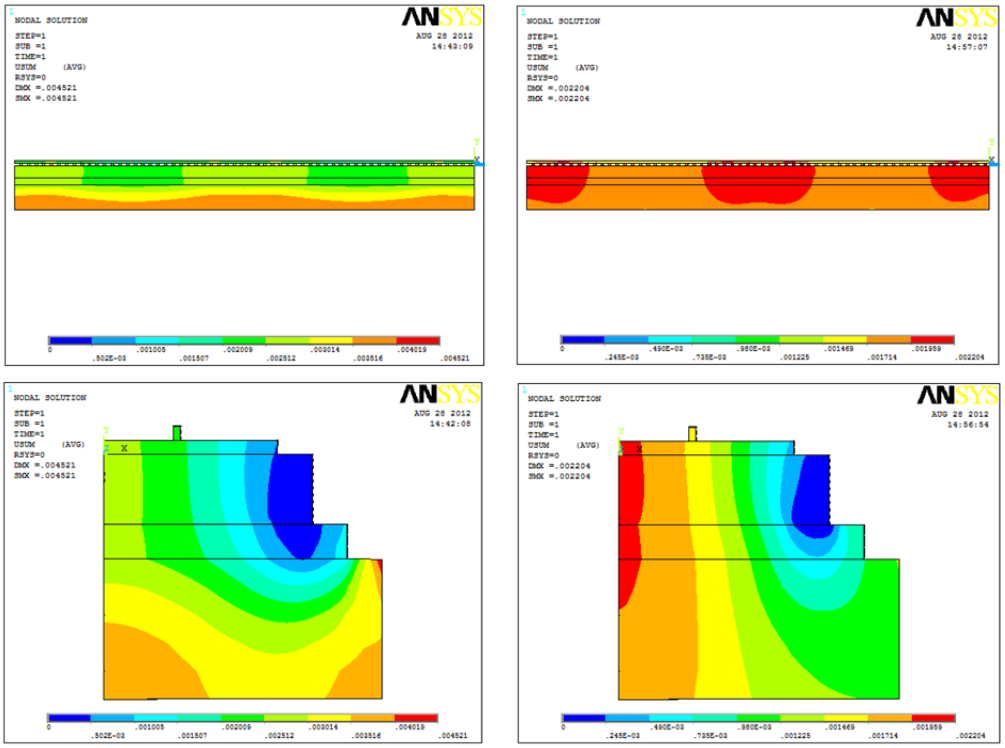


Figure 4.3: Magnitude of total displacements for the tare case: 1a - soft soil (left); 1b - stiff soil (right)

What can be noted it is that, in the case of a soft soil, the effect of the loading is recognisable well inside the structure, with a transmission of the load from the ballast to the sub-ballast to the subgrade. The higher deformations are localised in the ballast and sub-ballast. In particular with soft soil the sub-ballast layer thickness play an important role in distributing the loading to the underlying layers. In the case of soft soil, the structure is more vulnerable to larger deformations concentrated in the subsoil with risk of embankment reduced stability and failure of the shoulder of the embankment. In the case of stiff soil the embankment shows a greater stability with transmission of the load more in depth within the body of the structure. The case of the laden vehicle is not shown here for brevity, but it was observed an amplification of the behaviour observed at the lower loading level. Clearly the increase of axle load has a significant effect on the subsoil and this should be considered when programming a variation of traffic conditions on a track.

4.3 Dynamic Analyses

Dynamic analyses have been carried out starting from the findings from the static analyses and as an extension of such approach with the aim of investigating, through the interaction between the track and the train the effects of the train loading and train speed on the response of the track itself and of the different soil layers within the substructure. The following assumptions have been considered:

- As for the static analyses, a 3D mesh of elements has been considered in order to evaluate the three-dimensional stress/strain distribution within the structure;
- The RAIL_TRACK and RAIL_TRAIN modules, available in LS-Dyna, are applied for approximate modelling the train-track interaction and the calculation of the rail-wheel contact forces;

- the value of the wheel-rail contact stiffness has been set to 2 MN/mm (vertical and lateral stiffness can be specified) due to experimental measurements;
- Hughes-Liu beam elements (2-node elements) are used for the FE modelling of the rails;
- the wheel sets of the vehicle are explicitly modelled;
- the axle load is simulated as a set of vertical forces applied at the moving vehicle-rail contact points;
- Rail / wheel roughness can be implemented by load curves giving the vertical deviation of the rail surface from the theoretical centerline of the beam elements as a function of distance along the track / as distance of wheel surface away from perfect circle
- Various soils (loose and dense uniform sand and stiff/soft clay) are considered in the model to investigate the effect of the change of stiffness in the substructure

Moving from the findings of the static analysis and having acquired a good confidence with the numerical approach, the model prepared for the dynamic analyses has evolved with the aim of considering a real test case.

A section of the Bulgaria line which runs between the Serbian border (Kalotina in Bulgaria, by Dimitrovgrad in Serbia) and the Turkish border (Svilengrad in Bulgaria, by Kapikule in Turkey) was chosen. The traffic mix on this line is freight and passenger with a maximum speed of 100 km/h; freight traffic has a typical line speed of 75km/h. Data regarding the condition of the track for this section suggests the track is in bad condition and speeds may have to be reduced by up to 30% in order to counteract the condition of the track.

The modeled geometry refers to the cross section at km 253+200 of the line between Dimitrovgrad and Svilengrad. The elements and layers as modeled in LS-Dyna are depicted below.

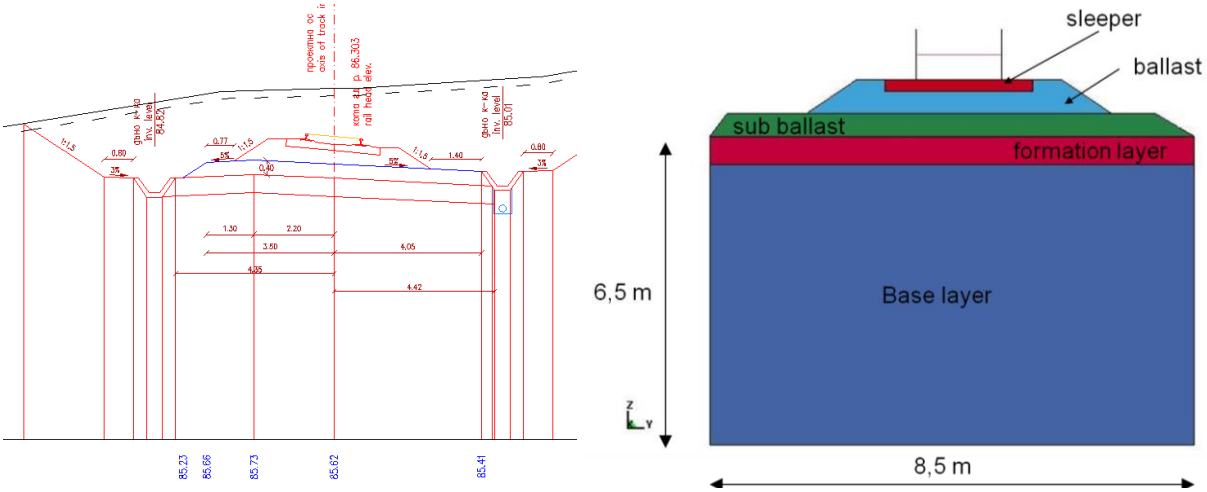


Figure 4.4: Geometry of the Cross section at Km 253+200 along the Dimitrovgrad-Svilengrad railway line in Bulgaria (left); section elements as modelled in LS-Dyna (right)

The modelled track is 100m in length and it is meshed with solid elements. A total of 150000 elements (solid tetra) is obtained. The model of the vehicle is also visualized.

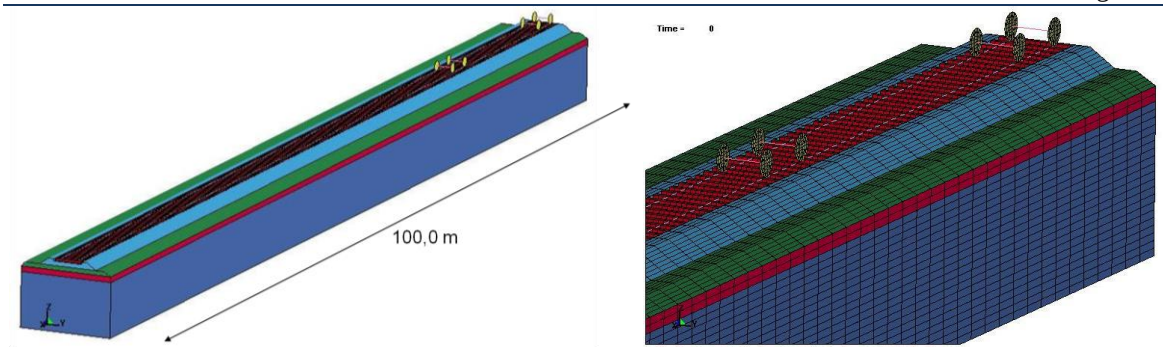


Figure 4.5: Longitudinal view of the cross-section: unmeshed geometry (left); meshed model (right)

A first dynamic analysis was carried out in the case of a laden vehicle, moving at constant speed of 120 kph, with a soft soil. The results in terms of stress field distribution in the different layers when the train is moving have been obtained and they are visualized below. These pictures clearly shows the footpath of the train wheels in the structure and the propagation and extension of the stress field in the soil layers. Indeed for a soft soil in the substrate (e.g. formation layer) evidence of the stress induced by the train is quite significant.

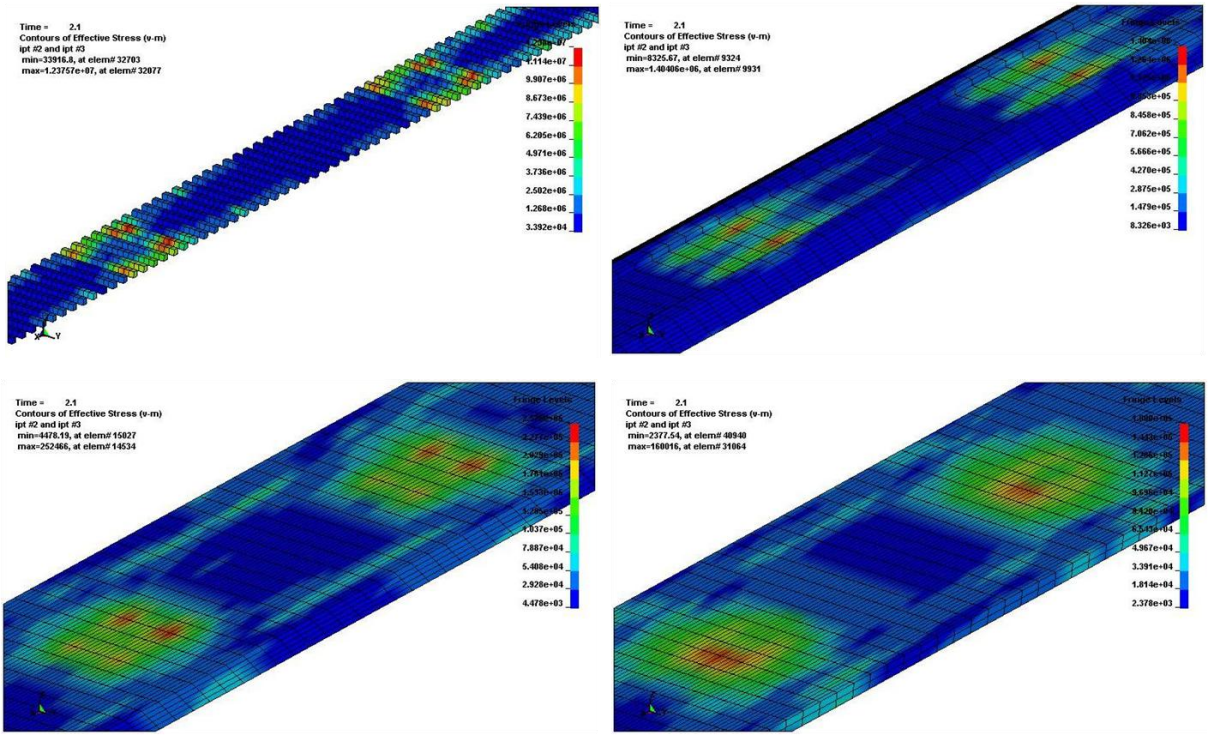


Figure 4.6: Dynamic analysis: contours of effective stress along time (e.g. following the train movements) in the different layers: sleepers (top left); ballast (top right); sub-ballast (bottom left) and substrate (bottom right)

The study has progressed towards the analysis of the dynamic effects induced in the track structure and substructure under different speed and axle load conditions and in combination with different soil types. Next Table reports the material properties used for the subsoil layer.

Table 4.3: selected soil materials used in the simulations and elastic constants

Material	Dry Density [kg/m^3]	Young Modulus (E) [MPa]	Bulk Modulus (K) [MPa]	Shear Modulus (G) [MPa]
Loose uniform sand	1470	18.0	15.0	6.9
Dense Uniform sand	1840	51.0	68.5	18.7
Stiff clay	1730	10.0	11.1	3.7
Soft clay	1330	2.5	1.4	1.0

Figure 4.7 reports the variation of the resultant accelerations at different depths below the track at a certain location along the track induced by the passage of the train.

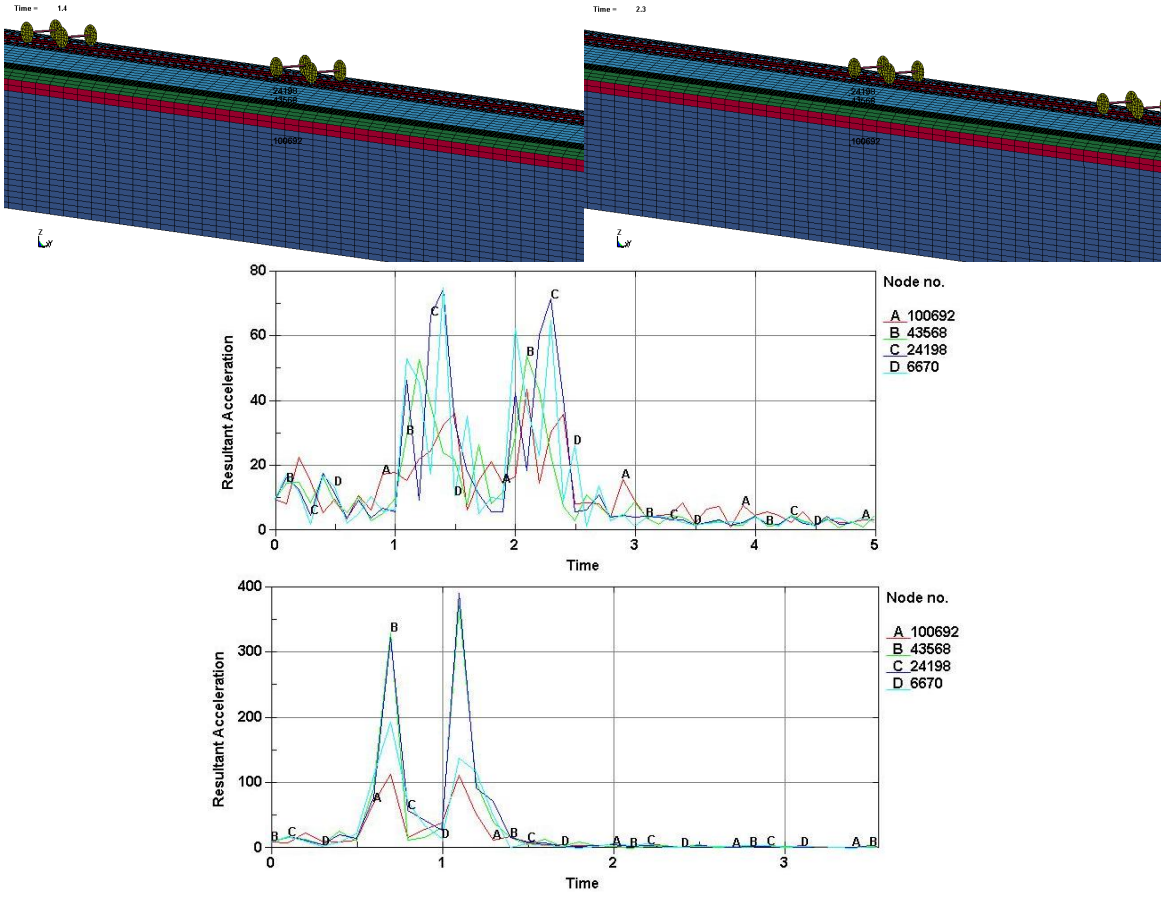


Figure 4.7: Variation of resultant accelerations at different depths below the track (A subsoil, B formation layer, C sub-ballast, D ballast) at a certain location along the track induced by the train travelling at speed V= 70km/h and axle load =10 t (above) and V=140 km/h and axle load = 22.5 t (bottom)

On the top of the figure the location of the selected 4 control nodes is visualized together with the wheelsets of the moving train above the selected control location. Note that the first bogie, when running at a speed of 70 km/h, arrives in correspondence of the control location at time 1.4 sec (after the start of the simulation) and the second bogie at 2.3 sec. The 4 control nodes are part of the ground layer (node A, number 100692), the formation layer (node B, number 43568), the sub-ballast (node C, number 24198) and the ballast (node D, number 6670). The first graph reported in Figure 9 shows the accelerations in the different layers during time, with the train moving at a speed of 70 km/h and with an axle load of 10 t. The upper values of accelerations are recorded in the upper layers (ballast and sub-ballast) in correspondence of the passage of the two individual bogies, at about 1.4 and 2.3 seconds. The second graph shows the accelerations measured at the same location and control nodes, but with a train

moving at higher speed (140 km/h) and with higher axle load (22.5 t). The effect of increased speed and axle load results in higher accelerations and peaks which are closer together, with accelerations in the ground layer which increase of almost 3 times.

Figure 4.8 shows the variation of the vertical contact force between wheel and rail in the two conditions of vehicle speed of 70km/h and axle load 10 t and vehicle speed of 140 km/h and axle load 22.5 t, with the track on a ground soil made of loose sand. Again the influence of speed and axle load is clearly evident, with closer peaks of contact force in correspondence of the sleepers at higher vehicle speed and maximum average contact force which is increased of about 2 times passing from a condition of lower speed and axle load to higher speed and full laden conditions.

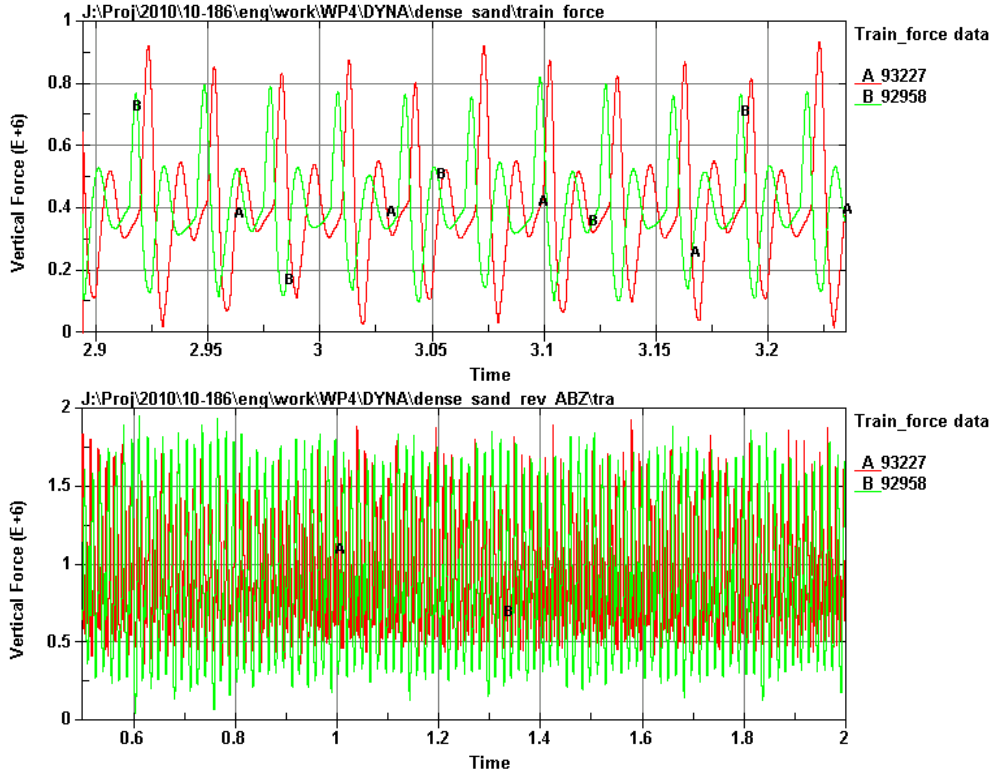


Figure 4.8: Wheel/track contact force along the track on loose sand as ground soil for different speed and axle load, V= 70km/h and axle load =10 t (above) and V=140 km/h and axle load = 22.5 t (bottom)

The next step in the study was the analysis of the influence of stiffness change in transition zones, where the stiffness of the track changes significantly over a short distance. Figure 4.9 shows a picture taken at the Faurei test track in Romania, which has been made available by the Romanian Railway Authority (AFER) to carry out measurements for the validation of the work done in the project. In particular the concrete bridge shown in the picture corresponds to one of the measurements location along the test track where a series of measures will be taken. On the right in Figure 4.9 a model representing a similar situation is shown. The model of the transition zone is based on the same layered structure of the previous model with the addition of the shoulder of the embankment, the abutment and the concrete bridge. The same approach was used for the analysis of the transition zone, with a simulation of the wheelset of the freight train passing over the bridge at various speeds and axle loads (see also Shi et. al., 2012, where a similar approach has been proposed). Figure 4.10 shows the distribution of effective stresses in the structure; one can observe that the higher stresses are localised in correspondence of the wheelset position and the most rigid elements of the model

(wheels , axles and sleepers). In the bottom picture of Figure 4.10 we can observe the complex stress distribution in the soil in the transition zone, when the wheelset is starting to enter into the bridge, above the abutment.

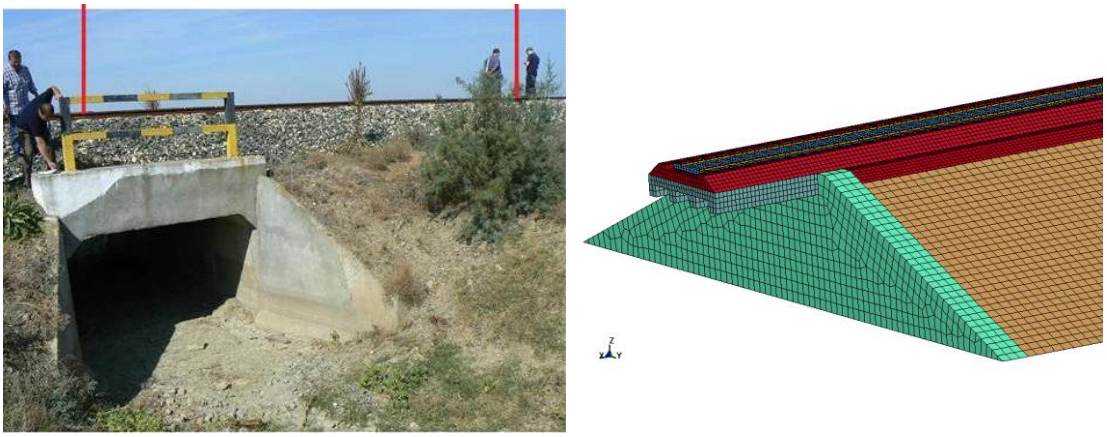


Figure 4.9: Analysis of bridge-embankment system

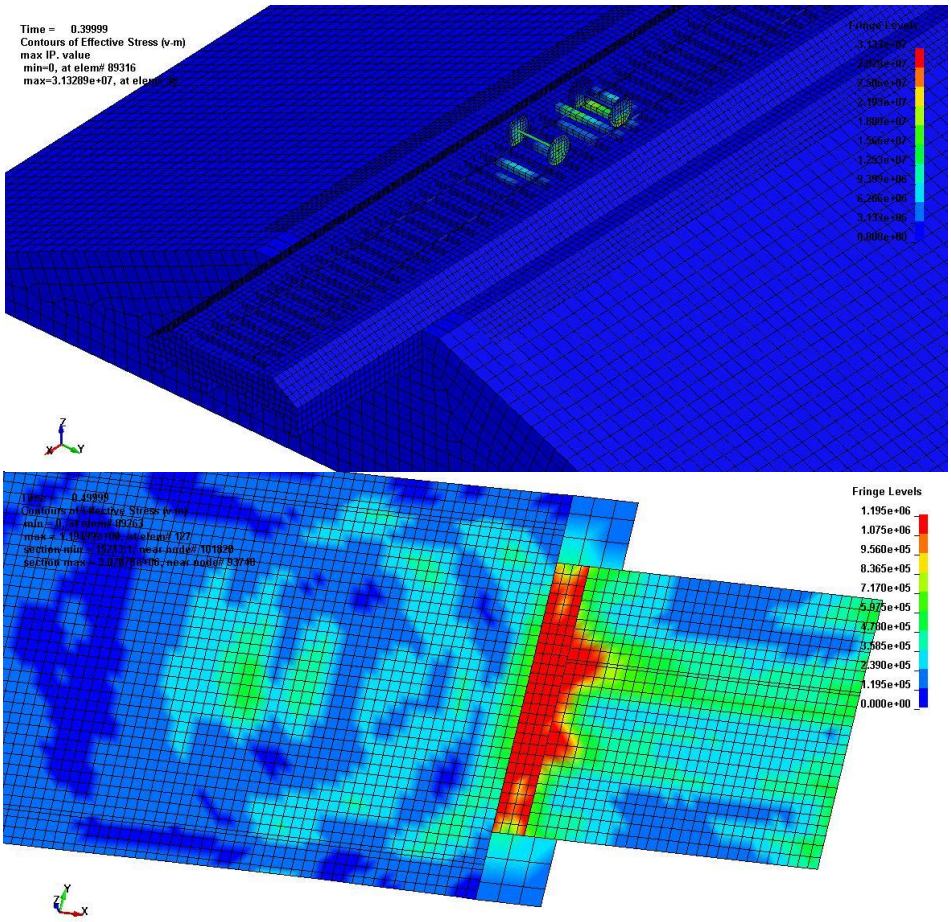


Figure 4.10: Distribution of effective stresses in the structure: stress concentrations are localised in correspondence of the individual wheelset position (above) and three-dimensional complex stress distribution is observed in the subsoil (below)

Similarly as above, it is of interest to quantify the effect of the train passage on the substructure. Figure 4.11 shows wheel/track contact force along the track and the variation of

resultant accelerations at different depths below the track (A subsoil, B formation layer, C sub-ballast, D ballast) at a location close to the transition zone. We can observe that in correspondence of the bridge we measure the highest contact forces which increase up to a factor 4 with respect to the values far from the transition area. Again the vertical accelerations increase in the substructure at the passage of the wheelset and increase significantly from the sublayer to the ballast.

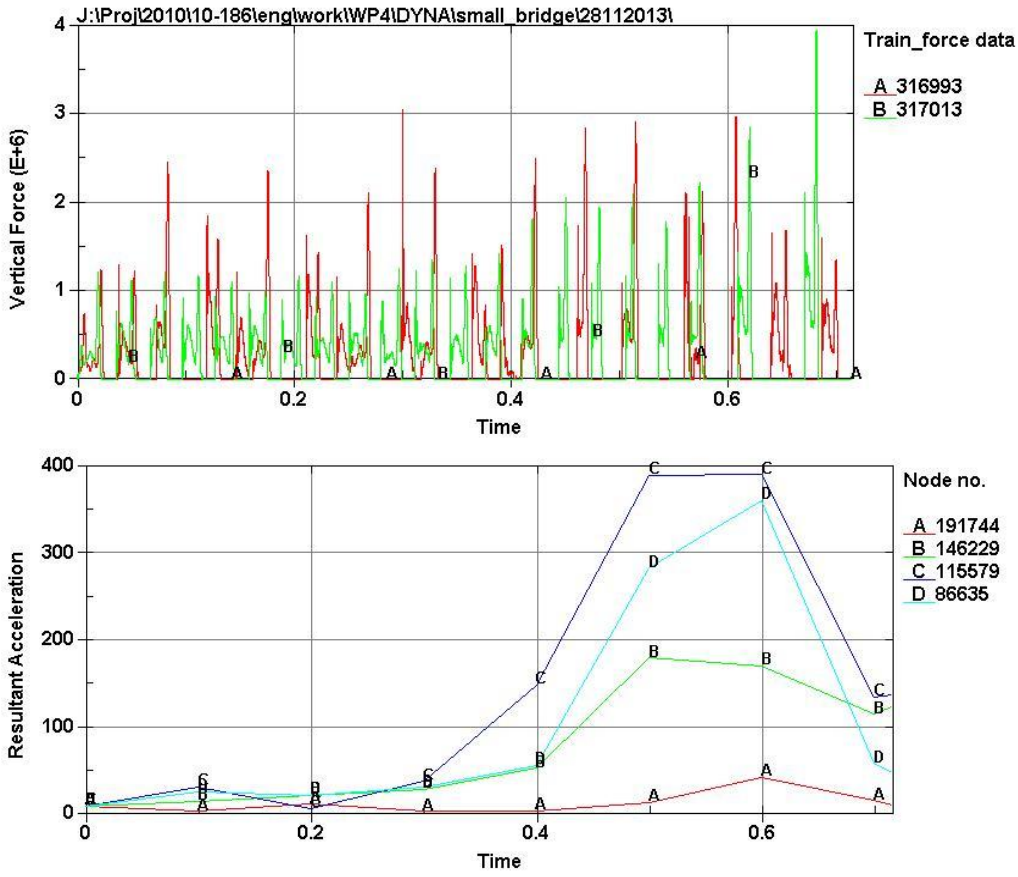


Figure 4.11: Wheel/track contact force along the track (above) and variation of resultant accelerations at different depths below the track (A subsoil, B formation layer, C sub-ballast, D ballast) (below) at a location close to the transition zone

4.4 Ground stabilization and monitoring technologies

The above results shows that increasing the axle load and speed of freight vehicles, there is a significant increase of the stress levels in the substructure, of contact forces at the wheel/rail interface and in terms of accelerations in the ground. In presence of soft subsoil it is important to quantify such effects and introduce strengthening measures.

The attention is towards the use of multifunctional geotextiles, able to provide both strengthening and monitoring functions (see Zangani, 2012). The classical use of geotextiles in embankments on relatively soft soils is to reduce settlement and to increase the bearing capacity and slope stability. Geotextiles are normally placed at the bottom of the embankment, about 50 cm above the original ground surface in one or more layers. In recent years a new kind of foundation, the so-called "geosynthetic-reinforced and pile-supported embankment" has been developed (Figure 4.13) and it is now in use in practice. Pile-like elements are placed in a regular pattern through the soft soil down to a load-bearing stratum

above which a reinforcement of one or more layers of geosynthetic (mostly geogrids) is placed before the embankment is filled. The stress relief in the soft soil results from an arching effect in the reinforced embankment over the pile heads and a membrane effect of the geosynthetic reinforcement.

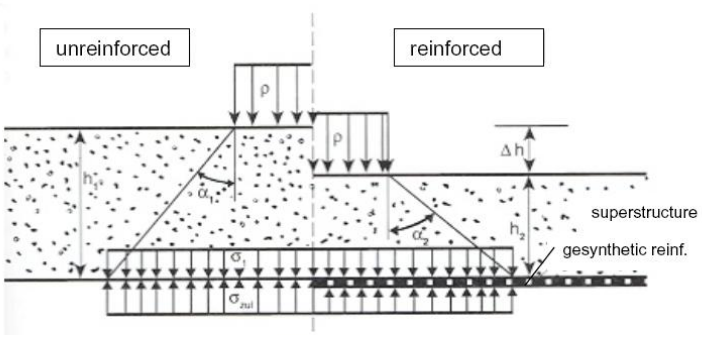


Figure 4.12: Use of geotextiles for soil reinforcement

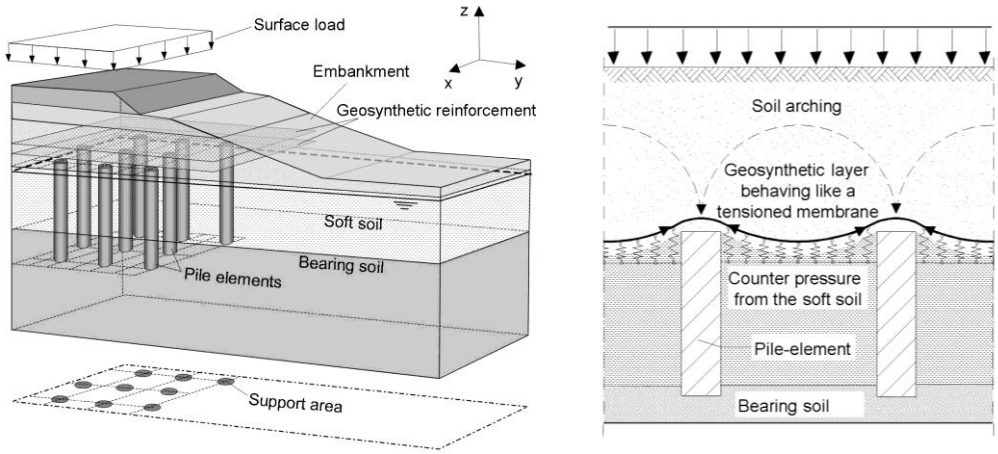


Figure 4.13: Geosynthetic-reinforced and pile-supported embankment

Up to date design and construction standards require the installation of systems to monitor the stability and serviceability of geotechnical structures. New multifunctional geotextiles are nowadays introduced in geotechnical engineering practice since they provide, at the same time, both the stability and monitoring functions. The multifunctional geotextile includes protection of the railway substructure against the increased loads induced by heavier vehicles travelling at higher speed by strengthening and stabilisation of the existing structures and the monitoring of their performance with the possibility of the infrastructure owner being alerted by an alarm before structural failure occurs. Figure 4.14 shows an example of prototype of multifunctional geotextile developed within the Polytect research project, which has been coordinated by the writer. Such kind of reinforcing and monitoring elements will be tested in Sustrail.



Figure 4.14: Multifunctional geogrid with embedded fiber optical distributed sensor (after POLYTECT)

4.5 References

J. Shi, M.PN Burrow, A. H.Chan, Y.J. Wang, 2012, "Measurements and simulation of the dynamic responses of a bridge-embankment transition zone below a heavy haul railway line", Proceedings of the Institution of Mechanical Engineers, Part F: Journal of Rail and Rapid

W Powrie, L. A. Yang, C. R. I. Clayton, 2007, "Stress changes in the ground below ballasted railway track during train passage", Proceedings of the Institution of Mechanical Engineers, Part F: Journal of Rail and Rapid Transit

D. Zangani, 2012, "Smart high performance materials for construction and geotextiles" Chapter 15 of book Smart high performance materials for construction, edited by Woodhead Publishing

5. UPGRADING SUBSTRUCTURE FOR HEAVIER LOADS

5.1 General

Bridges as substrates for heavier loads have been studied in the European Projects Sustainable Bridges (2007) and Mainline (2014). Some of the main outcomes will be summarized below.

5.2 Recommendations on assessment methods for bridges

Recommendations on assessment methods can be summarized in a procedure with three phases, see Figure 5.1:
Phase I - Start with as simple methods as possible
Phase II - If the results are not good enough, refine the methods (e.g. determine actual material properties, perform detailed calculations)
Phase III – If still not OK, use enhanced methods as

- Non linear finite element methods
- Reliability based methods
- Proof loading

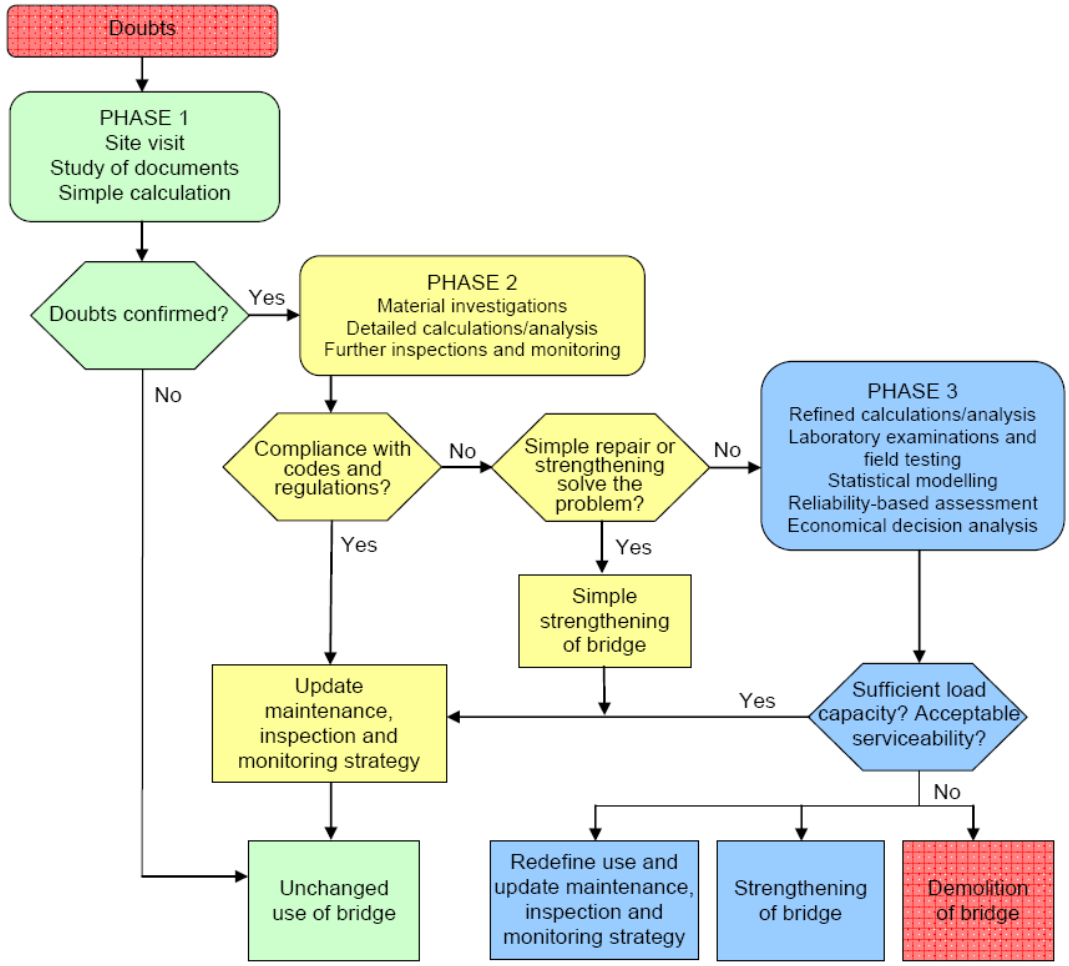


Figure 5.1: Three phases of Assessement of Bridges, SB-LRA, 2007

Inspection methods for bridges are treated in e.g. SB-ICA, 2007, in UIC 778-4R, 2009 and in Work Package 3 of MAINLINE, see Bharawaj et al., 2012. Degradation models are treated in Work Package 2 of MAINLINE, see Chryssanthopoulos et al. 2013. A data base for Swedish bridges and tunnels are given in BaTMan, 2012.

Assessment methods for bridges are treated in e.g. SB-LRA, 2007, Yanev, 2007, Cremona, 2011, and in Work Package 1 in MAINLINE, see Casas et al, 2013. An example of calibration of assessment methods by full scale testing to failure is presented by Puurula et al, 2012, 2013.

5.3 Recommendations on strengthening of bridges

The recommendations for strengthening procedures can be summarized in the following three steps:

Step I – Identify the material in the structure that needs strengthening
Step II – Identify the type of structure that needs strengthening
Step III –Chose a method for strengthening as e.g

- Carbon Fibre Reinforced Polymers (CFRP) laminate
- CFRP Near Surface Mounted Reinforcement (NSMF) Bars
- Prestressing

Some examples will now be given.

Strengthening methods using Carbon Fibre Reinforced Polymers, CFRP, are treated in e.g. Täljsten et al. 1994, 2006, 2011. Doctoral theses in this area have also been published by e.g. Carolin, 2003, Blanksvärd, 2009, and Sas, 2011. Three strengthening methods will now be exemplified. They have recently been tested on Swedish railway concrete trough bridges:

- Near Surface Mounted Reinforcement, NSMR

- Internal bonding of CFRP tubes

- Transverse internal post-tensioning

One problem with applying extra external reinforcement on the bottom of existing concrete bridges is that traffic passing below the bridge may scratch the reinforcement, see Figure 5.2.

One way of overcoming this is to use Near Surface Mounted Reinforcement, NSMR, which are glued into groves grinded into the concrete slab, see Figure 5.3. By installing FRP in mechanically produced grooves in the concrete surface, the bonding area increases (compared to traditional surface bonding) and a high interaction between the concrete and the FRP can be obtained. The bars are also better protected against external impacts when they are not completely exposed at the concrete surface.



Figure 5.2: High loads may scratch the bottom of concrete slabs as here on a bridge that was strengthened and tested to failure in Örnsköldsvik, Sweden. Photo by BAM, Berlin, Sustainable Bridges, 2007; SB7-3, 2008



Figure 5.3: Grooves are grinded in the bottom of a slab so that bars of Carbon Fibre Reinforced Polymers (CFRP) can be used as Near Surface Mounted Reinforcement (NSMR), SB7-3, 2008.

This method was tested on a reinforced concrete trough bridge in Örnsköldsvik some 500 kN north of Stockholm. The bridge was taken out of service in 2005 when a new high-speed railway line, the Botnia Line, was built. The bridge thus became available for testing to calibrate current code and assessment methods, Sustainable Bridges, 2007. The bridge was a frame bridge with two spans (~ 12+12 m), a slight longitudinal curvature (R = 300 m) and supports skewed with an angle of nearly 17 degrees (16º43').

The bridge was strengthened before the test with 18 (nine per beam) 10 m long NSMR bars of Carbon Fibre Reinforced Polymers, CFRP, each with a 10×10 mm cross section. The modulus of elasticity and the tensile strain at failure were 250 GPa and 0.8 %, respectively. The detailed design procedure of the NSMR strengthening is presented in SB7-3, 2008. The flexural capacity of the bridge was herby increased by about 30%.

The failure mode observed during the test was a flexural-shear failure, clearly showing that an interaction occurred between the shear and the bending mechanism. A computer model, using Brigade software (based on Abaqus), was developed to represent the response of the bridge during the test and calibrated using data from the test, which was then used to calculate the actual capacity of the bridge in terms of train loading using the current Swedish load model

which specifies a 330kN axle weight. These calculations show that the unstrengthened bridge could sustain a load 4.7 times greater than the current load model requirements (which is over 6 times the original design loading), whilst the strengthened bridge could sustain a load 6.5 times greater than currently required, see Figure 5.4, Puurula et al 2012, 2013.

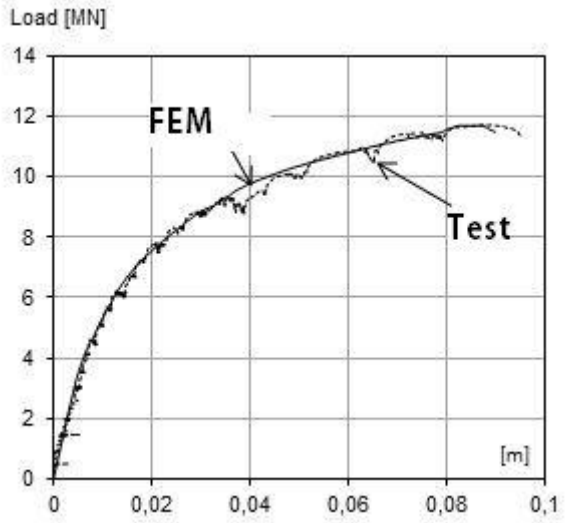


Figure 5.4: Load-deformation graphs according to the test and to the FEM model of the bridge in Örnsköldsvik, Puurula, 2012

5.4 Experience of tracks on bridges and transitions to bridges

Some experiences of tracks on bridges and transitions zones can be summarized as follows:

- Tracks on bridges can give extra strength to steel bridges
- Transition plates used on a steel truss bridge were not effective
- Under-sleeper pads seems to be a better solution

Some examples will now be given:

Transition plates used on a steel truss bridge at Sikån in northern Sweden were not effective – the bumps after installation were as big as before, Fara, 2014, see Figure 5.5, Figure 5.6, and Figure 5.7.

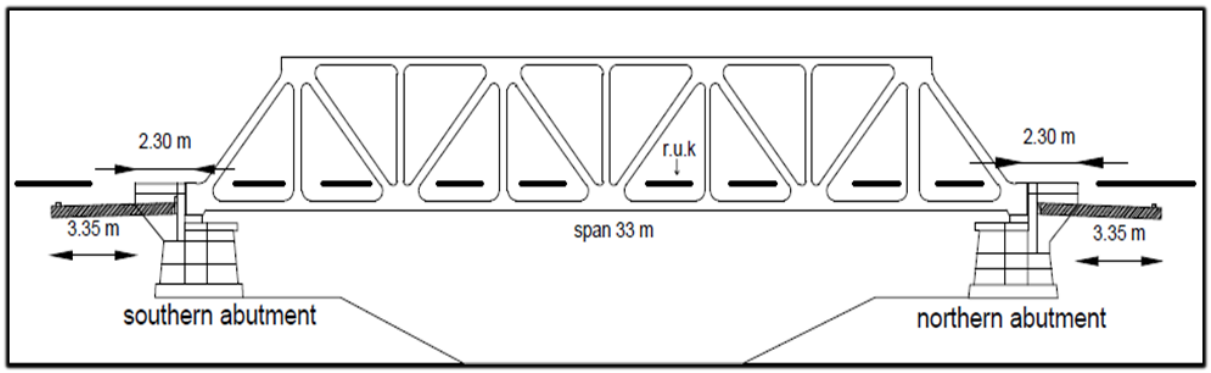


Figure 5.5: Transition slabs at Sikån Bridge, Fara, 2014



Figure 5.6: Installation of transition slab at Sikån bridge, Fara, 2014

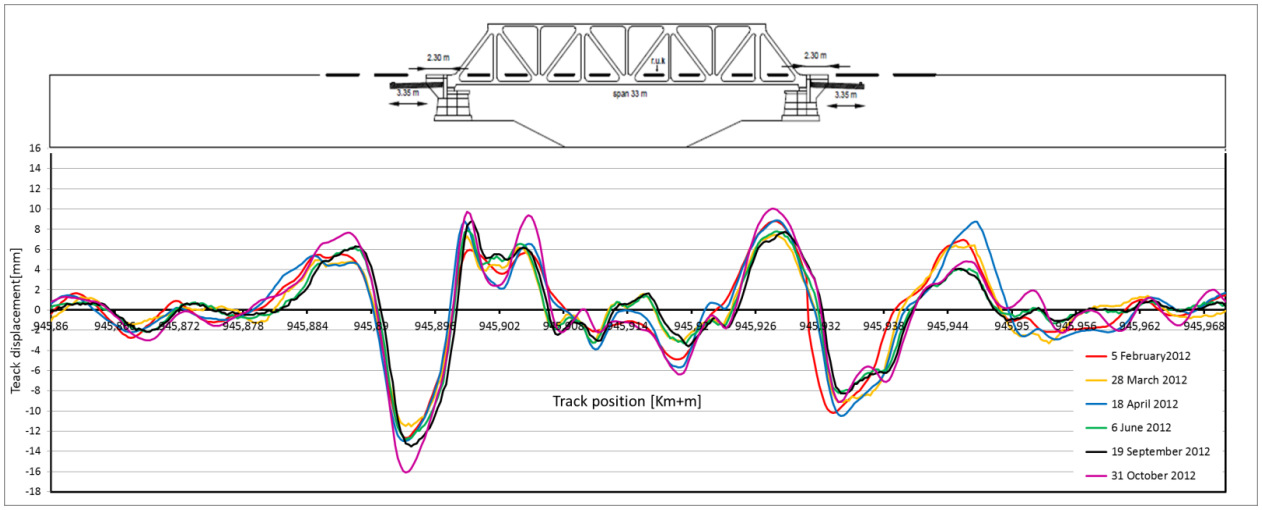


Figure 5.7: Measurements before and after installation of transition slabs at the sikån Bridge, Fara, 2014

5.5 References

BaTMan. 2012. *BaTMan – Bridge and Tunnel Management.* Data base of Swedish bridges and tunnels (In Swedish). https://batman.vv.se/batman/logon/logon.aspx?url=https://batman.vv.se/batman/

Bennitz, Anders. 2011. Externally unbonded post-tensioned CFRP tendons: a system solution. *Doctoral Thesis, Div. of Structural Engineering, Luleå University of Technology*.. http://pure.ltu.se/portal/da/publications/externally-unbonded-posttensioned-cfrp-tendons(f2ec06db-03e8-439f-ad12-94e73272c293).html

Bennitz, A., Täljsten, B., and Danielsson, G., 2012, CFRP strengthening of a railway concrete trough bridge – a case study, *Structure and Infrastructure Engineering*, Vol. 8, No. 9, September 2012, pp. 801-816.

Bharadwaj, U. et al. 2012. Report on assessment of current monitoring and examination practices in relation to degradation models *Mainline Deliverable D4.1*, 84 pp. http://mainline-project.eu/

Blanksvärd, Thomas. 2009. Strengthening of concrete structures by the use of mineral based composites: system and design models for flexure and shear. *Doctoral Thesis. Luleå University of Technology*, ISBN 978-91-86233-23-5, 156 pp.

Carolin, Anders. 2003. Carbon Fibre Reinforced Polymers for Strengthening of Structural Elements. *Doctoral Thesis 2003:18, Div. of Structural Engineering, Luleå University of Technology*, 194 pp. http://pure.ltu.se/portal/files/151462/LTU-DT-0318-SE.pdf

Casas, J.R. et al. 2013. Assessment methods for elderly rail infrastructure, *MAINLINE Deliverable 1.2.* http://mainline-project.eu/

CEN. 2000. prEN 10138-4:2000, Prestressing Steels – Part 4: Bars. CEN: European Committee for Standardization, Brussels, Belgium.

Chryssanthopoulos, M., et al. 2013. Degradation and intervention modelling techniques. *Mainline Deliverable D2.2*, 184 pp. http://mainline-project.eu/

Cremona, Christian. 2011. Structural Performance. Probability based assessment. London and New York: ISTE-Wiley, 448 pp, ISBN 978-1-84821-236-7.

Elfgren, L. et al. 2013. Benchmark of new technologies to extend the life of elderly rail infrastructure. *MAINLINE Deliverable 1.1.* http://mainline-project.eu/

Elfgren, L. et al. 2014. Guideline for application of new technologies to extend the life of elderly rail infrastructure. *MAINLINE Deliverable 1.4.* To be published.. http://mainline-project.eu/

Fara, Andrea, 2014. Transition Zones for Railway Bridges. A Study of the Sikån Bridge. M.Sc thesis Luleå University of Technology, Luleå, Sweden. Ca 250 pp, To be published

Innotrack. 2010. Innotrack – Innovative Track systems. *A European FP6 Integrated Research Project during 2006-2010*. Some 136 deliverables are available at www.innotrack.eu

MAINLINE, 2013. MAINtenance, renewaL and Improvement of rail transport iNfrastructure to reduce Economic and environmental impacts. *A European Community 7th Framework Program research project* 2011-2014 with 19 partners. Grant agreement 285121, SST.2011.5.2-6. Dr. Björn Paulsson, UIC/Trafikverket acts as Project Coordinator, see http//.mainline-project.eu

Nilimaa, Jonny. 2013. Upgrading concrete bridges: post-tensioning for higher loads. *Licentiate Thesis, Div. of Structural Engineering, Luleå University of Technology*, http://pure.ltu.se/portal/files/41761237/Jonny_Nilimaa.Komplett.pdf, 300pp.

Puurula, Arto. 2012. Load-carrying capacity of a strengthened reinforced concrete bridge. Non-linear finite element modeling of a test to failure. Assessment of train load capacity of a two span railway trough bridge in Örnsköldsvik strengthened with bars of Carbon Fibre Reinforced Polymers (CFRP). *Doctoral Thesis, Div. of Structural Engineering, Luleå University of Technology*, http://pure.ltu.se/portal/files/36697444/Arto_Puurula.pdf

Puurula, A, Enochsson, O, Sas, G, Blanksvärd, T, Ohlsson, U, Bernspång, L, Täljsten, B & Elfgren, L., 2013, Loading to failure and 3D nonlinear FE modelling of a strengthened RC bridge. *Structure & Infrastructure Engineering*. http://dx.doi.org/10.1080/15732479.2013.836546

Sas, Gabriel. 2011. FRP Shear Strengthening of Reinforced Concrete Beams. *Doctoral Thesis. Luleå University of Technology*, http://pure.ltu.se/portal/files/32725277/Gabriel_Sas_PhD_Thesis.pdf

SB-6.3-3, 2007.Strengthening of the Frövi Bridge. Report in the project Sustainable Bridges, 50 pp, www.sustainablebridges.net

SB-7.3, 2008. Field test of a Concrete Bridge in Örnsköldsvik, Sweden. Report in the project Sustainable Bridges, 415 pp, www.sustainablebridges.net

SB-D1.4. 2005. Railway Bridge Research. An overview of current research carried out in the Sustainable Bridges project. *Deliverable D1.2 compiled by Luleå University of Technology in the Sustainable Bridges project*. Available at the WP1 Section in http://www.sustainablebridges.net/

SB-ICA. 2007. Inspection and Condition Assessment. *Guideline developed in the EC-FP6 Project Sustainable Bridges*, 259 pp. www.sustainablebridges.net

SB-LRA 2007. Load and Resistance Assessment of Railway Bridges. *Guideline developed in the EC-FP6 Project Sustainable Bridges*. 428 pp. www.sustainablebridges.net

SB-MON. 2007. Guideline for Monitoring of Railway Bridges. *Guideline developed in the EC-FP6 Project Sustainable Bridges*, 93 pp. www.sustainablebridges.net

SB-STR. 2007. Guide for use of Repair and Strengthening Methods for Railway Bridges. *Guideline developed in the EC-FP6 Project Sustainable Bridges*. 139 pp. www.sustainablebridges.net

Smartrail. 2012. Smartrail - Smart Maintenance Analysis and RemediaTion of RAIL infrastructure. *A European FP7 Project 2011-2014 with 15 partners.* http://smartrail.fehrl.org/?m=1

Sustainable Bridges. 2007. Sustainable Bridges – Assessment for Future Traffic Demands and Longer Lives. *A European FP 6 Integrated Research Project during 2003-2007with 32 partners. Four guidelines and 35 background documents* are available at www.sustainablebridges.net

Sustrail 2012. Sustrail -The sustainable freight railway: Designing the freight vehicle – track system for higher delivered tonnage with improved availability at reduced cost. *A European FP7 project 2011-2015 with 29 partners from 13 countries.* www.sustrail.eu/

Täljsten, Björn. 1994. Plate Bonding. Strengthening of Existing Concrete Structures with Epoxy Bonded Plates of Steel or Fibre Reinforced Plastics. *Doctoral thesis 1994:152D. Div. of Structural Engineering, Luleå University of Technology, 2nd Ed 1994, 283 pp.*

Täljsten, Björn. .2006. FRP Strengthening of Existing Concrete Structures. Design Guideline. *Div. of Structural Engineering, Luleå University of Technology*, ISBN 91-89580-03-6, 1st Ed 2002, 4th Ed 2006, 228 pp.

Täljsten, B., Blanksvärd, T. & Sas, G. 2011. Handbok för dimensionering i samband med förstärkning av betongkonstruktioner med pålimmade fiberkompositer (Design Guideline for FRP Strengthening of Existing Concrete Structures. In Swedish). *Div. of Structural Engineering, Luleå University of Technology. ISBN 978-91-7439-146-6, 184 pp*

UIC 778-4R. 2009. Defects in railway bridges and procedures for maintenance. *UIC Code 778-4 R*, 1st Ed, July 1989, Revided 2009, International Union of Railways, Paris, 32 pp.

Yanev, Bojidar. 2007. Bridge Management, *New York: John Wiley & Sons*, 655 pp, ISBN 978-0-471-69162-4.

6. TRACK DEFECTS ANALYSIS

6.1 Introduction

Two aspects of track defect damage were considered: the effect of changing support stiffness and the effect of multiple cracks. These are reported in the next two subsections.

6.2 Stress in Rails subject to Varying Support Stiffness

6.2.1 Model

A simple Euler–Bernoulli beam model of the rail was used to investigate the effect of varying support stiffness. This is illustrated in Figure 6.1, where the piecewise cubic terms in the rail displacements have fourth derivative zero as required to be general solutions of the Euler-Bernoulli equation. The four coefficients of these terms are set by enforcing continuity of displacement and slope at the sleepers and by requiring that the ratios of moment to slope and of reaction force to displacement equal the specified stiffnesses.

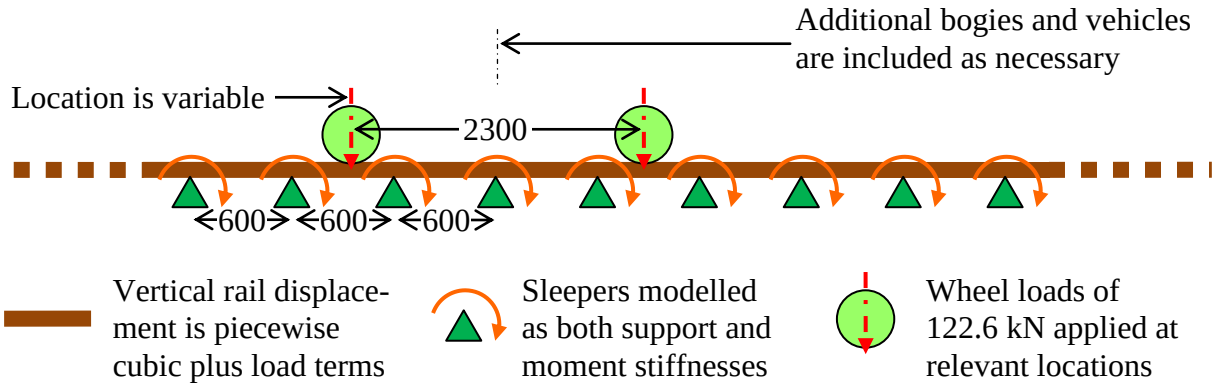


Figure 6.1: Beam model of rail

In this fast-running model each sleeper can have different stiffness properties. The model gives results almost identical to the traditional Winkler beam model[1] when the sleeper spacing is sufficiently small (and loading is between sleepers).

A failing of the simple model is that it assumes that the force required to push down into the ballast is the same as that required to lift rail by the same distance. In this work the model has been extended to include the effect of varying stiffness (different for upward and downward movement). This was done by initially using the downward values (which can be different for each sleeper), changing the stiffness of sleepers at which upward movement is predicted, and re-solving. Changing stiffness and re-solving needs to be repeated until all sleepers have the appropriate stiffness since directions of movement depend on the stiffnesses.

[1] In Winkler's approximation the individual sleeper stiffnesses are subsumed into a continuous foundation with a constant stiffness loading. The analytical solutions of the resulting equations have been widely used in railway design and analysis. Winkler, E.: "Vorträge über Eisenbahnbau" (Lectures on railway construction), Heft 1, 2, Verlag H. Dominicus, Prag (1867)

In the model positive bending moments (BM's) correspond to tensile stresses in the rail head and occur at sleeper locations while negative BM's correspond to tensile stresses in the rail foot and occur at wheel load locations. As vehicles move along track the magnitudes of the BM's change, normally being smallest when a wheel is directly over a sleeper.

6.2.2 Results

The effect of including non-linear stiffness is shown in Figure 6.2. These models have two 18m wagons with 25t axle-load standing on UIC60 rail[2] supported on sleepers at 600mm centres with a vertical stiffness, Kv, of 50kN/mm and a rotational stiffness of $Kv.W^2/12$=375 kNm/rad, for a sleeper width, W, of 300mm. For the non-linear (free) model the sleeper stiffnesses are both set to zero when the rail is lifting off the rail, while the non-linear (1/20) model has the stiffnesses reduced by a factor of 20.

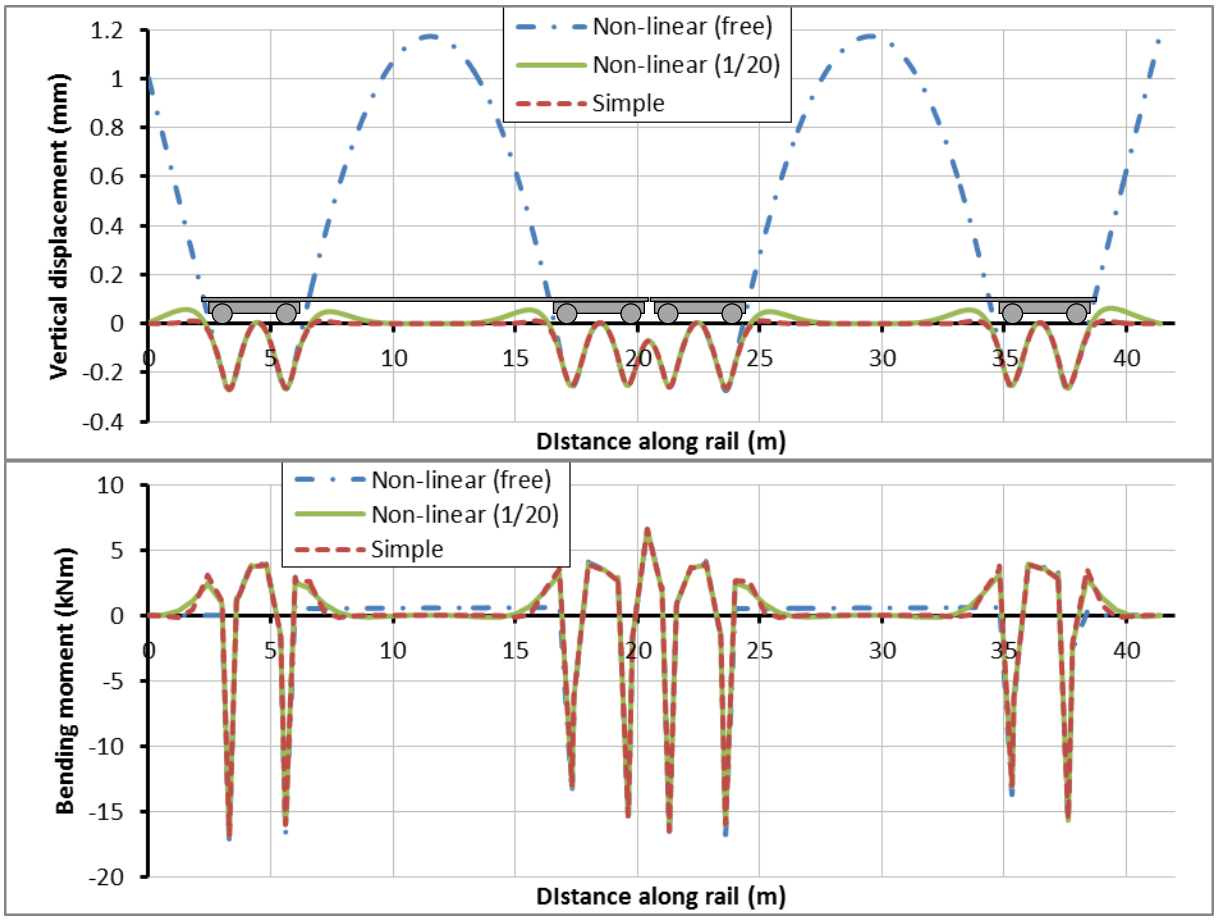


Figure 6.2: Comparison of simple and non-linear models of rail bending

It can be seen that there is little difference between the simple and 1/20 models; the BM's are particularly close. For the free model the rail lifts off the sleepers along the section between inner wheelsets of the vehicle body. The positive BM inboard of the inner wheelsets reduces as the upward stiffness decreases, but the largest two BM's (between wheelsets on a bogie and between vehicles) are unaffected. A small increase in the maximum negative BM at inner

[2] BSEN13674:1 "Railway applications. Track. Rail. Vignole railway rails 46 kg/m and above", British Standards Institution, 2011

wheelsets can be seen for the (free) model. For this UIC60 rail the stress at the rail head in MPa is given by 3 times the BM in kNm; the maximum tensile stress in these models is thus 20MPa (BM=6.7kNm) and occurs between two vehicles since the adjacent wheels are closest to each other. At the rail foot (since the neutral axis is not in the centre of the rail section) the relevant factor is 2.66, giving peak stresses of between 50MPa and 52MPa for the three models.

Note that as two vehicles (8 wheels) pass over a section of track each piece of the rail head experiences 11 tensile stress peaks.

If a sleeper has become unsupported, due to ballast settlement or damage then the displacements and BM's increase. This situation has been modelled and the results are shown in Figure 6.3 for the 'non-linear (1/20)' model. The largest displacements and BM's occur when the wheel is directly over the unsupported sleeper. Compared to the results shown in Figure 6.2 the maximum downward displacement and positive BM have both approximately doubled[3]; the maximum tensile stress is now 35MPa.

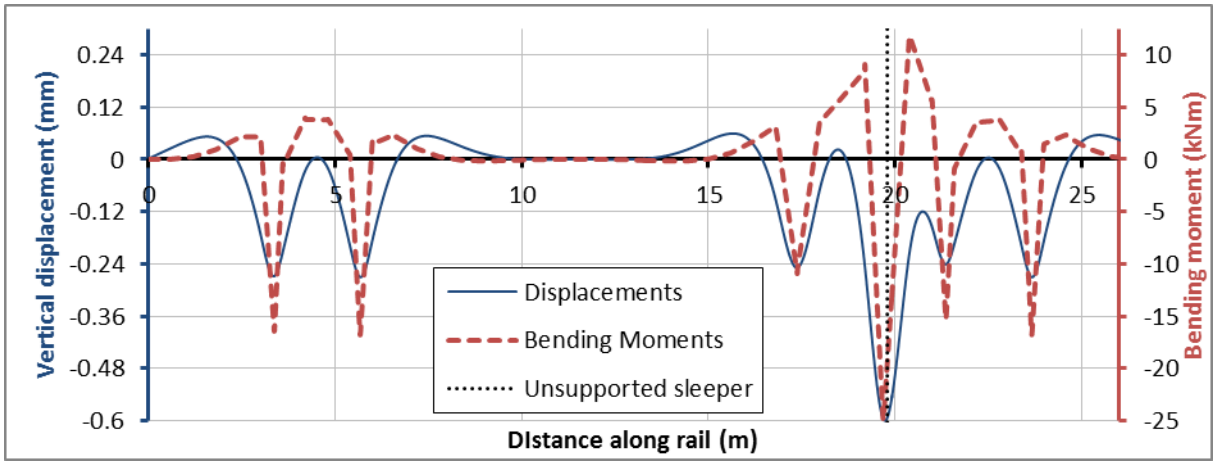


Figure 6.3: Rail bending when one sleeper is unsupported

The tensile stresses and downward displacements almost double again if two adjacent sleepers are unsupported; Figure 6.4 shows the results in this case. The BM of 21.3kNm corresponds to a tensile stress of 64MPa in the rail head. Note that in Figure 6.4 the peak stress occurs when the vehicles are at a different location on the track to Figure 6.3.

[3] This is consistent with the doubling calculated using a dynamic model of a wheelset passing over a three-dimensional model of track, pad, sleeper, ballast and subgrade reported in A Lundqvist and T Dahlberg. "Load impact on railway track due to unsupported sleepers". Proc IMechE, Part F: Journal of Rail and Rapid Transit, 219(2):67–77, 2005.

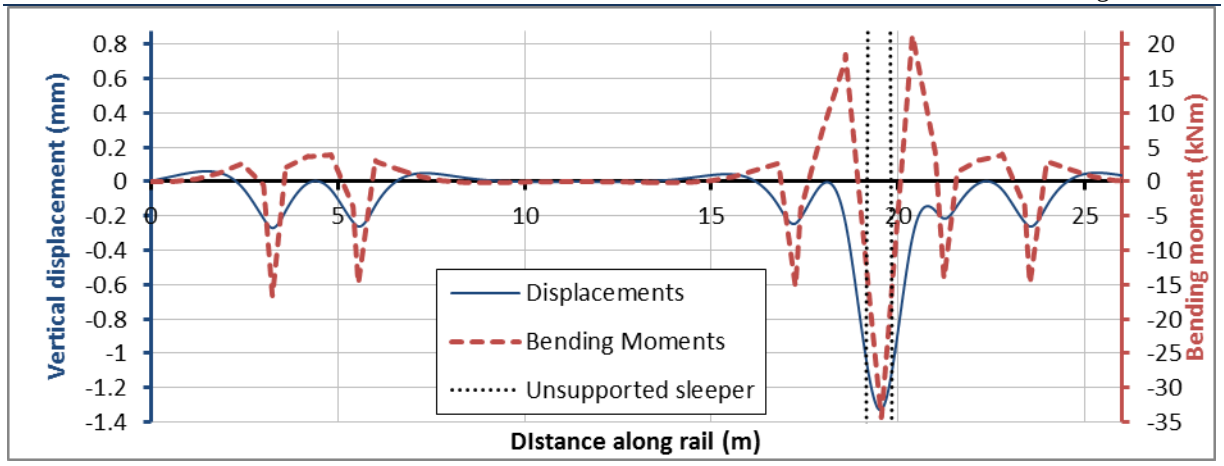


Figure 6.4: Rail bending when two sleepers are unsupported

To put these stresses in context, continuously welded rail in the UK is installed at a stress-free temperature of about 27°C; at 10°C the tensile stress would be 40MPa.

The stresses associated with transition onto a stiff foundation, e.g. passing over a culvert can be analysed with these models. Figure 6.5 shows that the displacements and BM's associated with a transition from the normal foundation (with a stiffness of 50kN/mm) to a one that is 20 times as stiff. Note that as this is a static model the results are the same whichever direction the vehicles are travelling. The BM at the first stiff sleeper is almost double the value associated with the uniform (normal) foundation for the vehicles in this location, 10.3kNm vs. 5.6kNm.

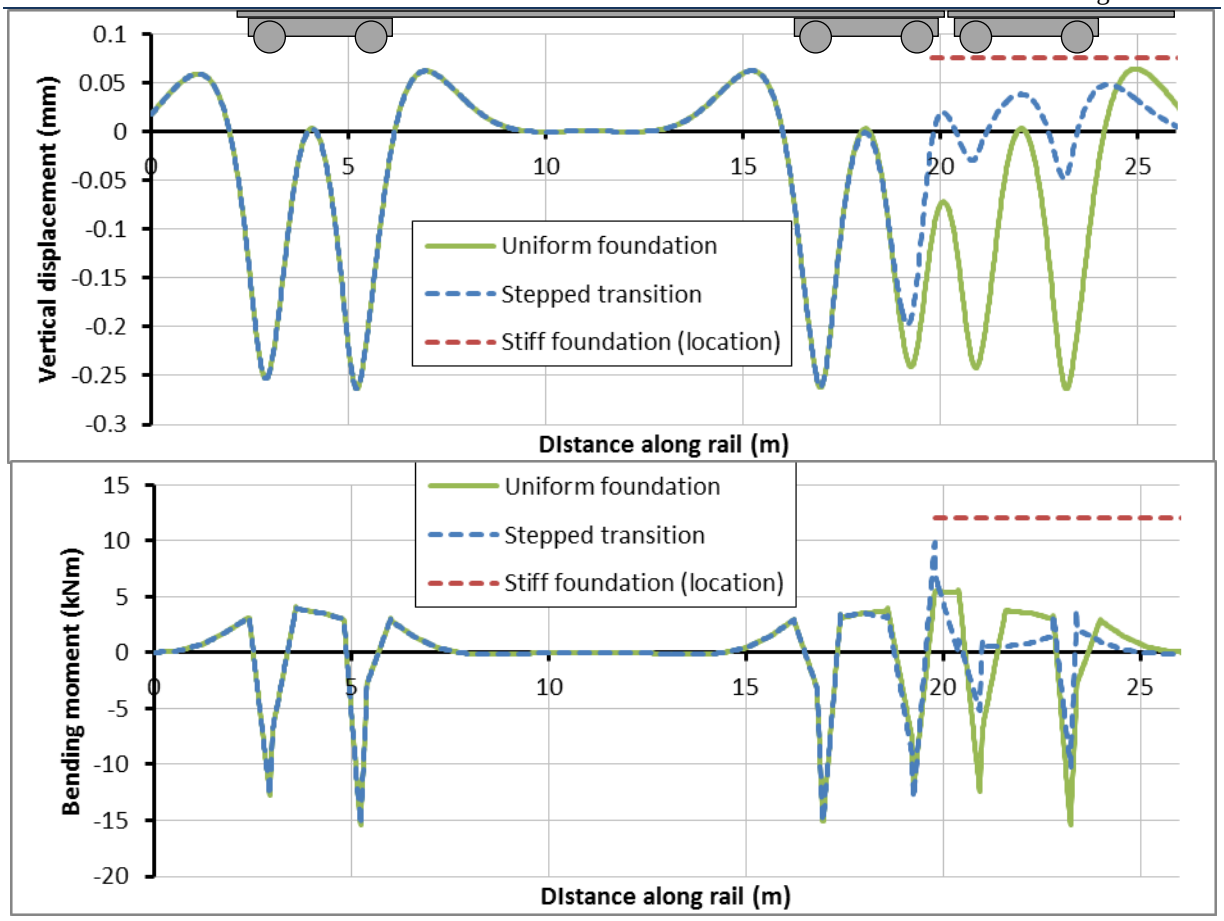


Figure 6.5: Vehicle passing over transition to stiff support

A more gradual change in support (foundation) stiffness is known to be less damaging. It was found that if the stiffness for the end sleeper of stiff foundation was 100kN/mm instead of 1000kN/mm the BM increased to only 8.1kNm (see Figure 6.6). This doubling of the normal stiffness was found to produce a better transition to 20 times the stiffness than did ten, or five times the stiffness.

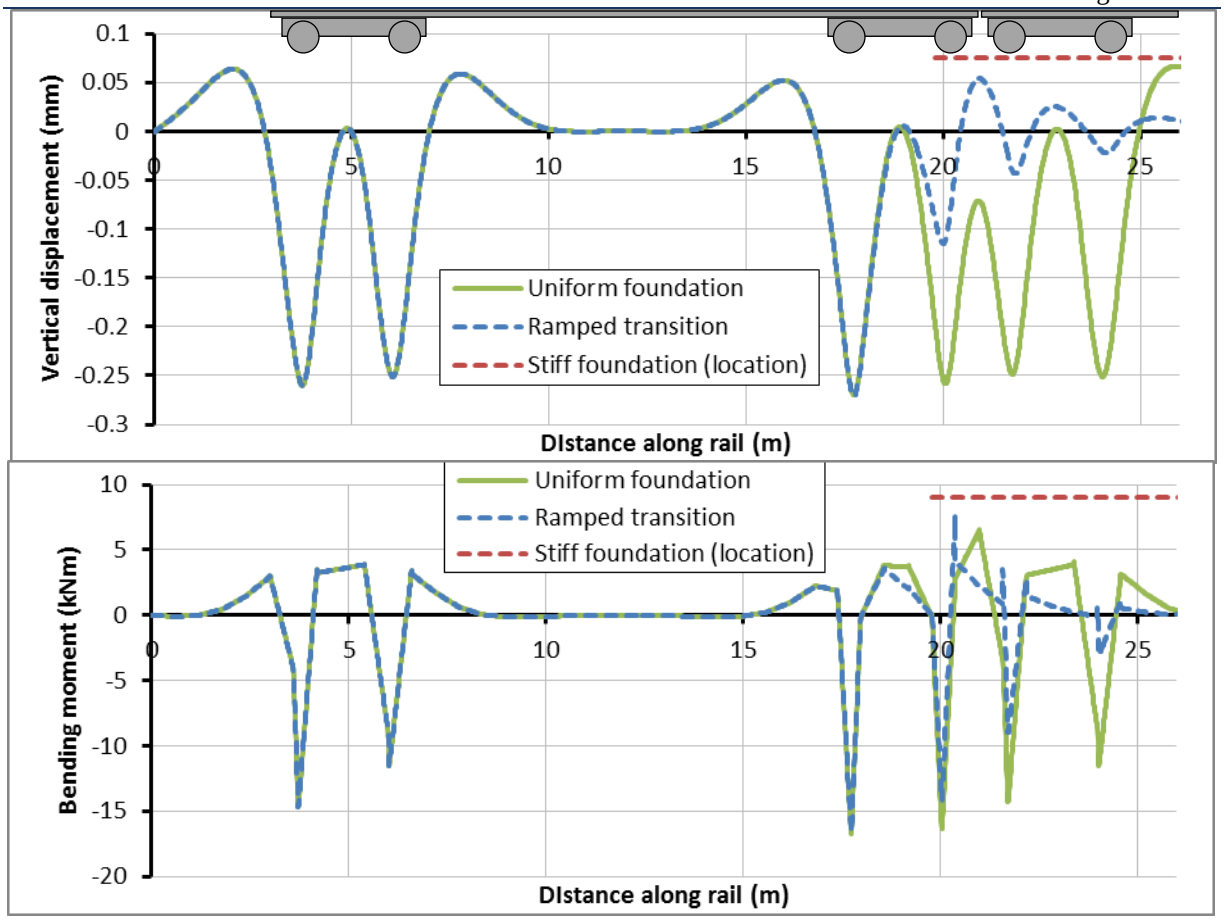


Figure 6.6: Vehicle passing over ramped transition to stiff support

6.2.3 Rail Bending Conclusions

The non-linear behaviour of foundation stiffness at sleeper locations has been incorporated into a fast-running model of rail track. It has been shown that this has a negligible effect on the bending moments predicted by the model.

A key finding of the model(s) is that the tensile stress in the rail between vehicles is over 50% larger than that between wheels on a bogie, so this location should be used to give conservative calculations of bending stress (many models consider a wheel, bogie, or vehicle in isolation so miss this peak value).

The model has been used to study how an unsupported sleeper and a transition onto a bridge could affect the bending stresses in rail:

- It was found that tensile stress could almost double if there is one unsupported sleeper and almost double again if there are two.
- This static model predicted that the transition results in a 50% increase in the tensile stress, but even a short (one sleeper-length) ramping of stiffness significantly reduced the peak value. It is emphasised that this is a static model and including dynamic effects would indicate that a far longer transition zone[4] is needed to adequately control the rail stresses.

[4] Tests in USA used 7.6m long transitions (D. Read and D. Li, "Design of Track Transitions", Research Results Digest 79, Transportation Research Board, 2006), while some Dutch track has 4m transitions (B Coelho, P Hölscher, J Priest, W Powrie, and F Barends, "An Assessment of Transition Zone Performance", Proc. IMechE, Part F: Journal of Rail and Rapid Transit, 2011 225: 129-139)

6.3 Multiple Cracks

6.3.1 Introduction

Rolling contact fatigue (RCF) cracks in rails are a major concern to infrastructure managers. Measures to mitigate RCF are expensive and include rail grinding, applying friction modifiers, restricting traffic speeds, and applying higher track access charges to more damaging vehicles.

Most models of RCF crack growth consider only single cracks; whereas RCF damage normally consists of large numbers of cracks (see Figure 6.7 for examples).



Figure 6.7: Examples of RCF damage from Railtrack's "Rail Failure Handbook" RT/CE/S/057, 2001

The fundamental parameter used in linear elastic fracture mechanics to predict both crack growth, and material fracture is the stress intensity factor (SIF). This parameter, conventionally denoted K, defines the stress field near to the crack and has three components corresponding to the three stress components acting on the crack face: Ki is associated with the normal stress (opening mode), while Kii and Kiii are associated with the two directions of shear stress, perpendicular and parallel to the crack tip.

6.3.2 Model

The BEASY boundary element software[5] was used to calculate stress intensity factors (SIF's) for a range of models of the railhead as shown in Figure 6.8. A two-dimensional model of a section of 102mm along the rail was created. The model considered the rail head; UIC 60 rail[6] has a head that is 51mm deep. For shallow cracks remote from wheel-rail contact a uniform tensile stress was considered appropriate[7].

[5] BEASY Boundary Element software, (www.beasy.com)

[6] BSEN13674:1 "Railway applications. Track. Rail. Vignole railway rails 46 kg/m and above", British Standards Institution, 2011

[7] The base of the head only experiences about 44% of the maximum bending stress seen at the top of the rail (section height 172, neutral axis height 80.92). However, the crack tip (with a length of 5mm) experiences a stress that is 95% of the maximum bending stress and relevant material (up to twice the crack depth) experiences only a 5% variation in stress by using uniform instead of a varying stress. Rail is installed in track at a higher temperature than that at which trains operate so experiences tensile thermal stress; thus, in operation, the variation in stress for 5mm-deep cracks would normally be less than 5%.

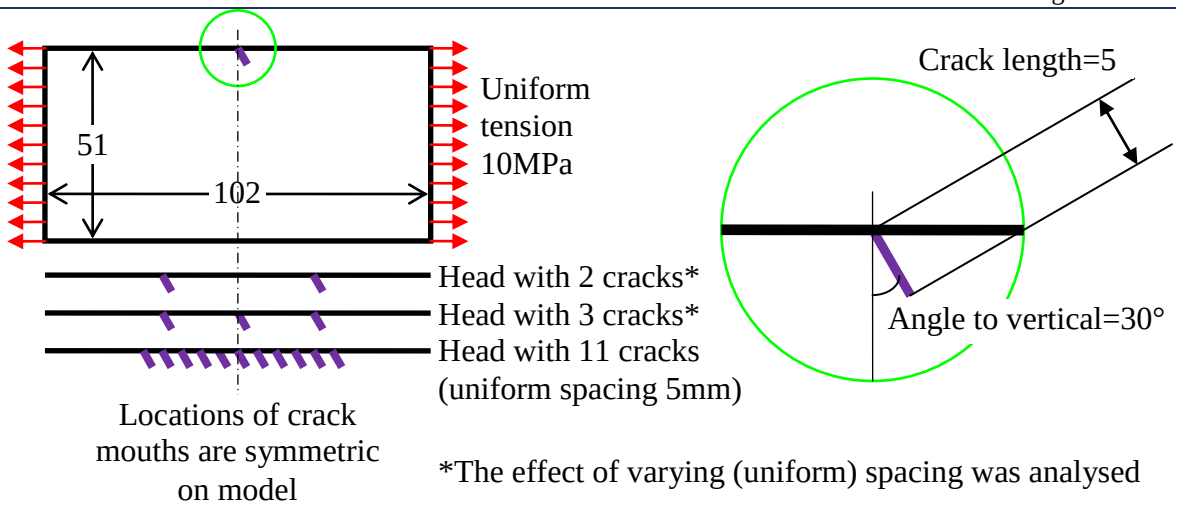


Figure 6.8: Crack models

The SIF's reported here were computed using J-integrals[8]. The model was validated and a sufficiently fine mesh established by comparison with standard solutions[9]. A comparison between SIF's calculated using J-integrals with those calculated by extrapolating crack opening displacements was also undertaken and showed very good agreement, though precise results depended on the choice of extrapolation.

A further comparison was made with the results for a 10mm radius crack in rail subjected to a 4kNm bending moment; the work reported here was intended to complement this earlier "comparator" work[10]. The results are shown in Figure 6.9 where is can be seen that the results from this fast-running two-dimensional model provide good indications of what would be expected from the far-slower three-dimensional model.

[8] Rice, J.R. "A path independent integral and the approximate analysis of strain concentration by notches and cracks", Trans. ASME, J. Appl. Mech., 1968, 35, 379-386. For a linear elastic material with Young's modulus E and Poisson's ratio v the SIF, K, and J-integral, J, satisfy $J=K^2(1-v^2)/E$.

[9] "Handbook of Stress-intensity Factors", Sih, G.C. and Lehigh University. Institute of Fracture and Solid Mechanics, 1973

[10] Fletcher,D. I.,Hyde, P., and Kapoor, A. "Growth of multiple rolling contact fatigue cracks driven by rail bending modelled using a boundary element technique". Proc. IMechE, Part F: J. Rail and Rapid Transit, 2004, 218(F3), 243–253

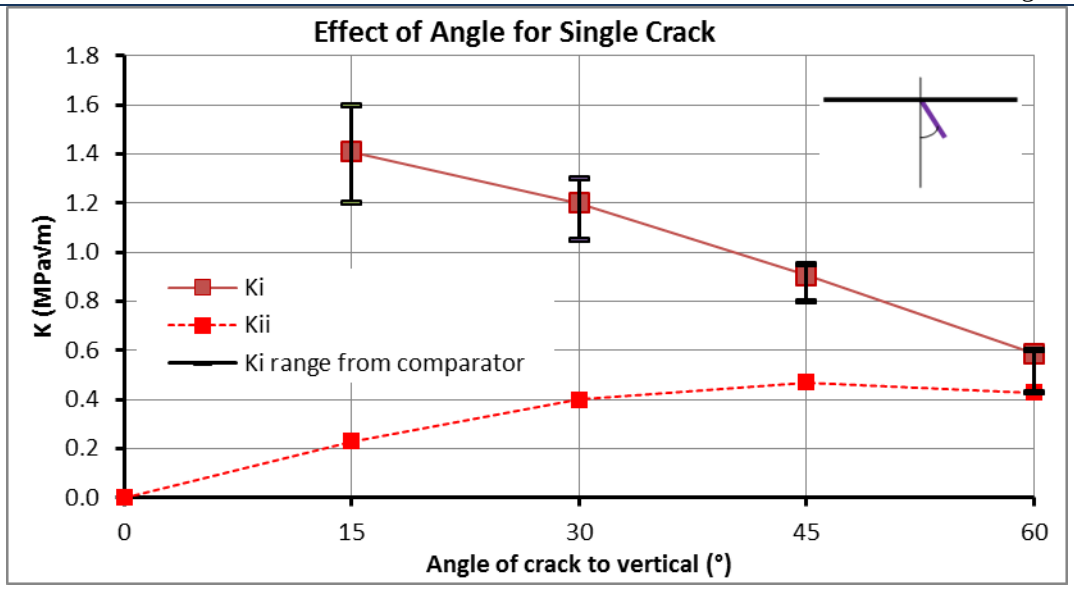


Figure 6.9: Stress intensity factors for single cracks at different angles

6.3.3 Results

The effect of changing crack separation on SIF's can be seen in Figure 6.10 for the left-hand end of a crack-group, Figure 6.11 for the middle crack, and Figure 6.12 for the right-hand end of a crack-group. Each plot includes results for a single crack and for groups of two (if appropriate), three, and eleven cracks. By comparing SIF's for one crack with other results it can be seen that even a spacing of 20mm is sufficient for a crack to be shielded by a neighbouring crack (to its right) leading to a 10% reduction in its SIF (Ki). For the right-hand end of a crack group the same level of shielding requires a spacing of about 12.5mm. For the end cracks the SIF is almost independent of the number of cracks (more than one).

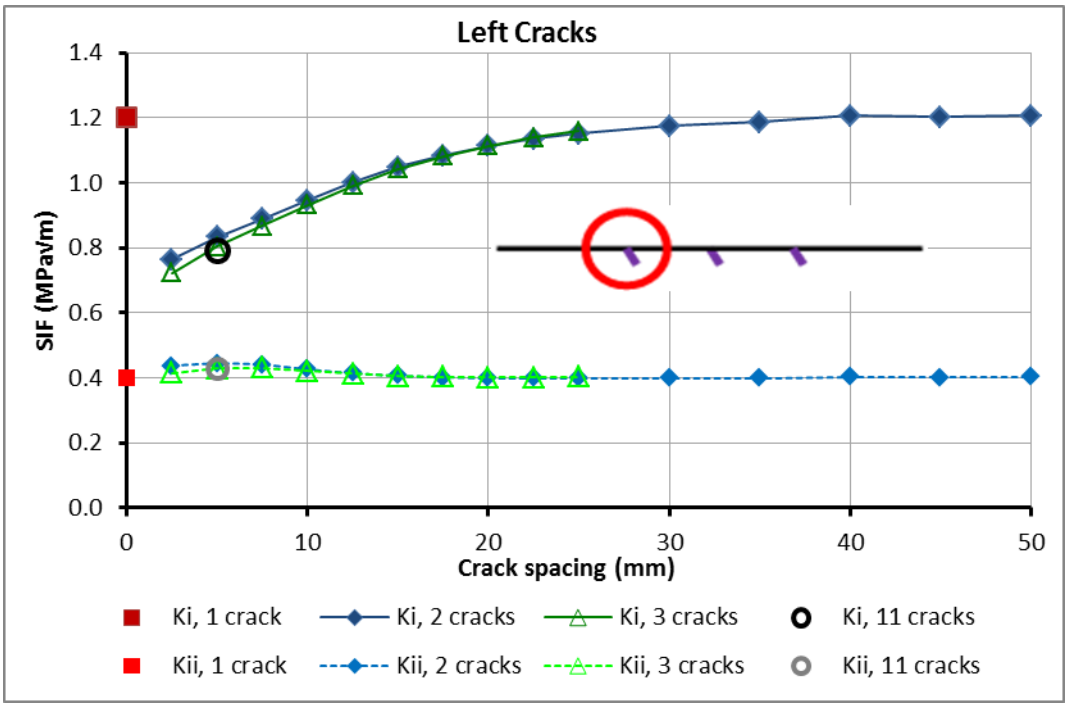


Figure 6.10: Stress intensity factors for cracks at left-hand end of group

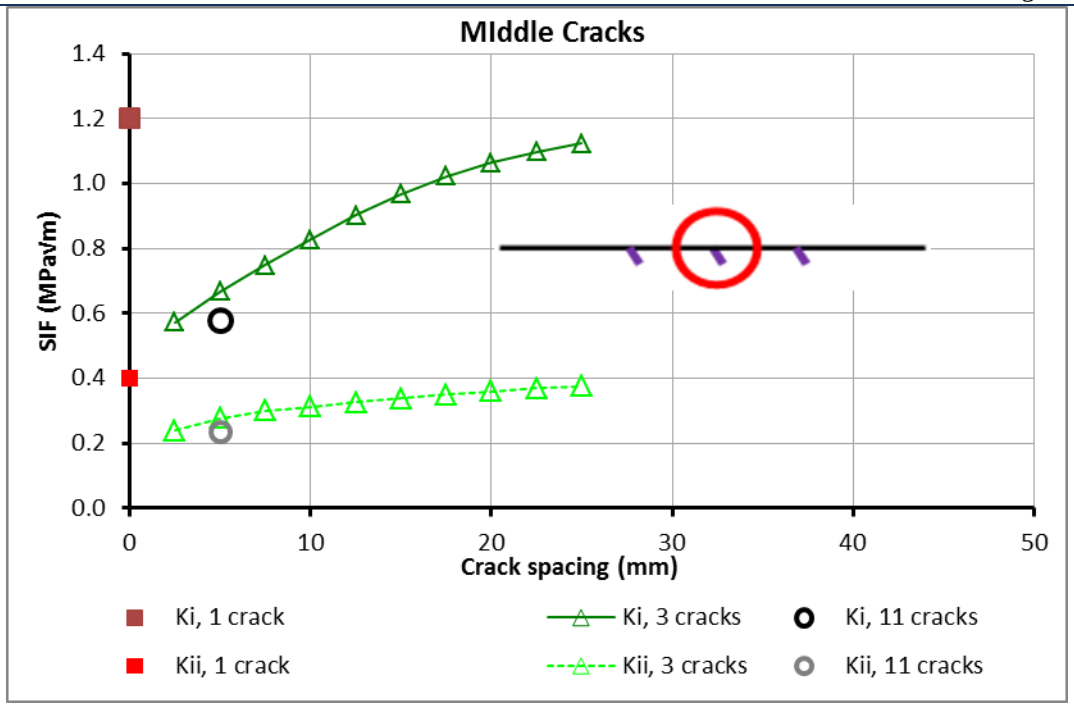


Figure 6.11: Stress intensity factors for cracks in middle of group

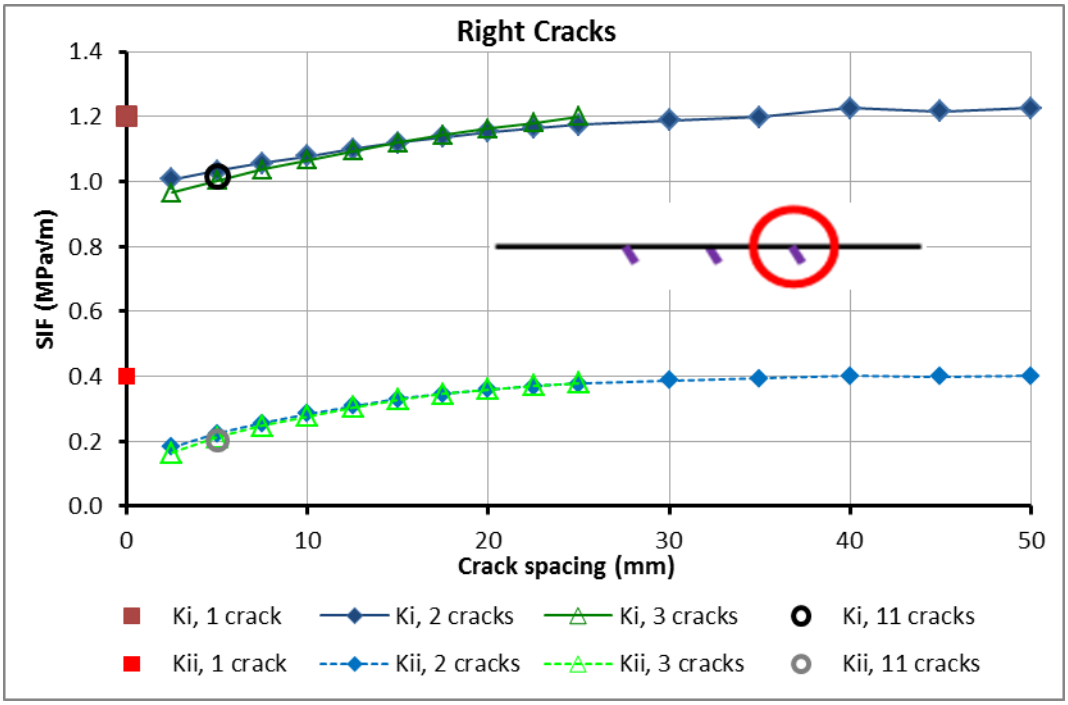


Figure 6.12: Stress intensity factors for cracks at right-hand end of group

The SIF's were calculated for each crack in the group of eleven. The results are shown in Figure 6.13. It is seen that the SIF's are almost constant away from the ends of the group.

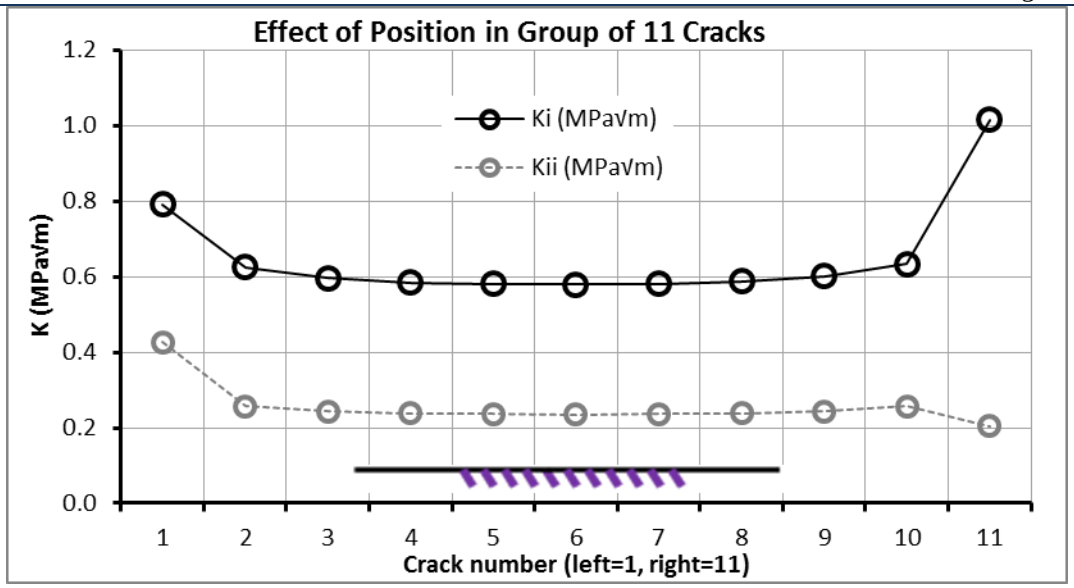


Figure 6.13: Stress intensity factors for cracks in group of eleven

6.3.4 Multiple Crack Conclusions

The analyses presented here have confirmed that the stress intensity factors associated with cracks away from the ends of crack groups are significantly lower (about half for 5mm separation) than those for isolated cracks.

The new results here are those for Kii which show the same halving as Ki (reference in Footnote 10).

Stress intensity factors associated with long wavelength crack growth can be approximated by multiplying the SIF results from this Section by 0.3 times the tensile BM's given in Section 6.2.

6.4 Conclusions

The effect of vertical plane long wavelength rail bending on rolling contact fatigue crack growth has been studied using two tools: rail bending using an analytic model of a beam supported on discrete sleeper (displacement and moment) supports; and a boundary element model of multiple crack growth.

It was found that

- the peak tensile stress in a rail head could occur between vehicles, a location that is often not included in more sophisticated models
- including non-linear stiffness of supports has a relatively small effect on rail stresses
- changes in stiffness associated with hanging sleepers or bridge abutments produce significant changes in stress (up to double)
- a one-sleeper transition is all that is needed to halve the increase in stress associated with a bridge abutment (but vehicle speeds were not considered)
- for cracks away from the ends of crack groups both the tensile-mode (Ki) and shear-mode (Kii) stress intensity factors are halved, compared to isolated cracks, when 5mm-long cracks are separated by less than about 5mm

7. CONCLUSIONS

The work of Task 4.2 "Supportive ballast and substrate" was focused on studying the key characteristics of the track and the substructure which need to be considered to reduce track geometry degradation, and contributing to optimisation of LCC. Poor trackbed stiffness and stiffness variation in transition zones and track defects such as multiple cracks and varying support stiffness were identified as key elements. Numerical methods based on FEM and BEM were developed and are available to address such aspects and to be applied to real cases such as those selected within SUSTRAIL. Additionally portable tools for monitoring train-track interaction and strengthening methods for bridges and transitions zones to bridges are proposed to upgrade the substructure for heavier loads.